

1 Design and implementation of multiplexed amplicon sequencing panels to serve genomic 2 epidemiology of infectious disease: a malaria case study

3 Emily LaVerriere^{1,2¶}, Philipp Schwabl^{1,2¶}, Manuela Carrasquilla^{1,2,3¶}, Aimee R. Taylor^{2,4}, Zachary M.
4 Johnson^{1,2}, Meg Shieh^{1,2}, Ruchit Panchal^{1,2}, Timothy J. Straub^{1,2}, Rebecca Kuzma^{1,2}, Sean Watson¹,
5 Caroline O. Buckee⁴, Carolina M. Andrade⁵, Silvia Portugal^{3,5}, Peter D. Crompton⁶, Boubacar Traore⁷,
6 Julian C. Rayner⁸, Vladimir Corredor⁹, Kashana James¹⁰, Horace Cox¹¹, Angela M. Early^{1,2}, Bronwyn
7 L. MacInnis², Daniel E. Neafsey^{1,2*}

8 Affiliations:

9 ¹ Department of Immunology and Infectious Diseases, Harvard T.H. Chan School of Public Health,
10 Boston, MA, USA.

11 ² Infectious Disease and Microbiome Program, Broad Institute of MIT and Harvard, Cambridge, MA,
12 USA.

13 ³ Max Planck Institute for Infection Biology, Berlin, Germany.

14 ⁴ Department of Epidemiology, Harvard T.H. Chan School of Public Health, Boston, MA, USA.

15 ⁵ Centre of Infectious Diseases, Parasitology, Heidelberg University Hospital, Heidelberg, Germany.

16 ⁶ Malaria Infection Biology and Immunity Section, Laboratory of Immunogenetics, National Institute of
17 Allergy and Infectious Diseases, National Institutes of Health, Rockville, MD 20852, USA

18 ⁷ Mali International Center of Excellence in Research, University of Sciences, Technique and Technology
19 of Bamako, BP 1805, Point G, Bamako, Mali.

20 ⁸ Cambridge Institute for Medical Research, University of Cambridge, Cambridge CB2 0XY, United
21 Kingdom

22 ⁹ Departamento de Salud Pública, Facultad de Medicina, Universidad Nacional de Colombia, Bogotá,
23 Colombia

24 ¹⁰ Guyana National Malaria Control Program, Ministry of Health, 0592 Georgetown, Guyana

25 ¹¹ Guyana Vector Control Services, Ministry of Health, 0592 Georgetown, Guyana

26 ¶ These authors contributed equally to this work.

27 * Corresponding author. Email: neafsey@hsph.harvard.edu

28 Keywords: malaria, genotyping, genome, epidemiology, relatedness, amplicon sequencing

29 **Abstract**

30 Multiplexed PCR amplicon sequencing (AmpSeq) is an increasingly popular application for
31 cost-effective monitoring of threatened species and managed wildlife populations, and shows strong
32 potential for genomic epidemiology of infectious disease. AmpSeq data for infectious microbes can
33 inform disease control in multiple ways, including measuring drug resistance marker prevalence,
34 distinguishing imported from local cases, and determining the effectiveness of therapeutics. We describe

35 the design and comparative evaluation of two new AmpSeq assays for *Plasmodium falciparum* malaria
36 parasites: a four-locus panel ('4CAST') composed of highly diverse antigens, and a 129-locus panel
37 ('AMPLseq') composed of drug resistance markers, highly diverse loci for measuring relatedness, and a
38 locus to detect *Plasmodium vivax* co-infections. We explore the performance of each panel in various
39 public health use cases with *in silico* simulations as well as empirical experiments. We find that the
40 smaller 4CAST panel performs reliably across a wide range of parasitemia levels without DNA
41 pre-amplification, and could be highly informative for evaluating the number of distinct parasite strains
42 within samples (complexity of infection), and distinguishing recrudescence infections from new infections in
43 therapeutic efficacy studies. The AMPLseq panel performs similarly to two existing panels of comparable
44 size for relatedness measurement, despite differences in the data and approach used for designing each
45 panel. Finally, we describe an R package (paneljudge) that facilitates design and comparative evaluation
46 of AmpSeq panels for relatedness estimation, and we provide general guidance on the design and
47 implementation of AmpSeq panels for genomic epidemiology of infectious disease.

48 **Introduction**

49 Genetic data are a valuable resource for understanding the epidemiology of infectious disease.
50 The value of this data type has been highlighted by the COVID-19 pandemic, for which viral sequence
51 analysis has greatly informed patterns of disease spread and evolution, influencing public health policy
52 decisions around the world (Oude Munnink et al., 2021). Applications of genetic data in epidemiology
53 extend from viral and bacterial outbreak management (Baker, Thomson, Weill, & Holt, 2018; Coll et al.,
54 2017; Quick et al., 2016) to the study of eukaryotic parasites underlying important diseases such as
55 malaria, toxoplasmosis, helminthiasis, leishmaniasis and Chagas disease.

56 Many use cases (applications) of genetic data have been identified for malaria (Dalmat,
57 Naughton, Kwan-Gett, Slyker, & Stuckey, 2019), the leading parasitic killer worldwide (WHO, 2019),
58 include tracking the spread of drug/insecticide resistance genetic markers and diagnostic resistance
59 mutations (Chenet et al., 2016; Jacob et al., 2021; Kayiba et al., 2021; Lautu-Gumal et al., 2021; Miotto
60 et al., 2020), assessing disease transmission levels (Daniels et al., 2015; Galinsky et al., 2015),

61 identifying sources of infections and imported cases (Liu et al., 2020; Tessema et al., 2019), and
62 estimating genetic connectivity among different populations (Taylor et al., 2017). Malaria parasite genetic
63 data also have demonstrated utility in therapeutic efficacy studies, for distinguishing recrudescence
64 infections potentially indicative of low drug efficacy from reinfections or relapses from dormant liver
65 stages (Gruenberg, Lerch, Beck, & Felger, 2019; Jones et al., 2021). In the malaria field, these
66 applications are served by different types of genetic data produced at varying resolution, technical
67 complexity, and cost, ranging from genetic panels that may comprise as few as 8 – 12 polymorphic
68 microsatellites (MS) or 24 single nucleotide polymorphisms (SNPs) (Baniecki et al., 2015; Daniels et al.,
69 2008), to whole genome sequencing (WGS) data (Miotto et al., 2015; Takala-Harrison et al., 2015).

70 To be scalable and sustainable, genetic data should be produced at the minimum resolution that
71 provides robust support for the intended analysis application. Whole genome sequencing (WGS) data
72 provide the most complete population genomic perspective on an organism of interest. However, the cost
73 and technical challenges of generating, storing, and interpreting WGS data are impediments to scalability
74 and widespread implementation for organisms with large genomes, or microbes with small genomes in
75 samples dominated by host DNA. Targeted sequencing approaches that focus deep coverage on select
76 genomic regions of interest using multiplexed PCR amplification (AmpSeq) are finding increased
77 application in conservation genomics and fisheries biology (Baetscher, Clemento, Ng, Anderson, &
78 Garza, 2018; Hargrove, McCane, Roth, High, & Campbell, 2021; Natesh et al., 2019; Schmidt, Campbell,
79 Govindarajulu, Larsen, & Russello, 2020), and can serve genomic epidemiology of infectious diseases by
80 focusing sequencing coverage on the most informative regions of pathogen or parasite genomes, instead
81 of typically dominant host genomes (Jacob et al., 2021; Tessema et al., 2020).

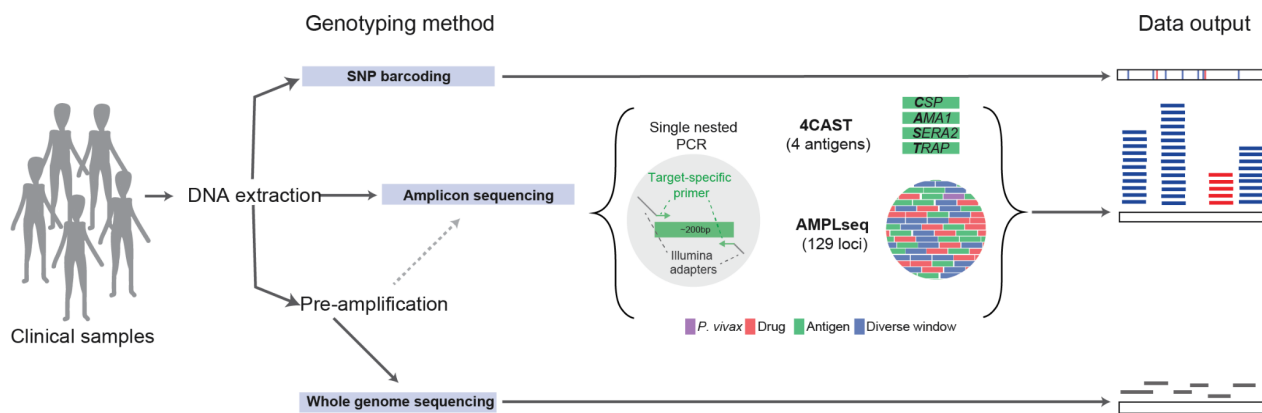
82 Recent work on AmpSeq protocols for genotyping malaria and trypanosomatid parasites has
83 confirmed the viability of this approach with low-parasitemia host and vector samples, where parasite
84 DNA comprises a very small fraction of the total sample (Jacob et al., 2021; Schwabl et al., 2020;
85 Tessema et al., 2020). Furthermore, one recent study has confirmed the value of designing amplicons to
86 capture multi-SNP 'microhaplotypes', which exhibit polyallelic rather than biallelic diversity to facilitate
87 relatedness inference (Tessema et al., 2020). New relatedness-based analytical approaches for genomic

88 epidemiology are currently developing for malaria parasites and other sexually recombining pathogens
89 (Henden, Lee, Mueller, Barry, & Bahlo, 2018; Schaffner, Taylor, Wong, Wirth, & Neafsey, 2018). The use
90 of genomic data for estimation of recent common ancestry shared by pairs or clusters of parasites or
91 mosquitoes has shown strong potential to provide epidemiologically useful inferences over very small
92 geographic distances (10s-100s of kilometers) and short time scales (weeks to months) relative to
93 traditional population genetic parameters of population diversity and divergence (Cerqueira et al., 2017;
94 Taylor et al., 2017). While many analyses of recent common ancestry in malaria parasites to date have
95 used WGS data, targeted genotyping of as few as 200 biallelic SNPs or 100 polyallelic loci (e.g.,
96 microsatellites or microhaplotypes) may also be used to infer recent common ancestry with necessary
97 precision (Taylor, Jacob, Neafsey, & Buckee, 2019), making AmpSeq an excellent candidate to serve
98 relatedness estimation.

99 However, there remains uncertainty in the molecular epidemiology field as to the suitability of
100 existing panels for profiling parasite or pathogen populations in specific geographic locations that did not
101 inform the original panel designs, and it is unclear which protocol features are most conducive to
102 implementation in both high and low resource settings. Should each disease field adopt a common
103 multiplexed amplicon protocol and panel, or should bespoke panels be implemented regionally to
104 address genetically distinct parasite populations and specific use cases?

105 To address these questions, in this manuscript we describe the design and comparative
106 evaluation of two new multiplexed amplicon assays for *Plasmodium falciparum* malaria parasites: a
107 four-locus panel composed of highly diverse loci, ideal for estimating the number of genetically distinct
108 strains within an infection (Complexity of Infection; COI) as well as distinguishing pre-existing vs. new
109 infections in any geographic setting, and a 129-locus panel composed of drug resistance markers and
110 many diverse loci for relatedness inference designed for application in South America (a region that did
111 not inform previously published panel designs) as well as other geographic regions. Both assays use
112 non-proprietary reagents (including standard PCR oligos) in order to maximize accessibility and
113 affordability in malaria-endemic regions. The panels are supported by new open-source bioinformatic
114 analysis pipelines to facilitate widespread use. We also show that the core sets of multiplexed PCR

115 oligos can flexibly accommodate most new targets not included in the original design, allowing for panel
116 customization towards detecting locally relevant resistance markers, polymorphic loci, and co-infecting
117 parasite species. We use whole genome sequencing data to explore the degree to which our newly
118 described and previously published genotyping panels can serve studies in diverse geographies, versus
119 the alternative of customizing panels with targets that are locally informative but not globally useful. We
120 suggest there is value in genotyping panels that can be flexibly adapted to incorporate informative
121 targets from pathogen populations of interest. The analyses and resources described in this manuscript
122 clarify the rapidly diversifying options for targeted microbial sequencing (**Fig. 1**), by providing tools and
123 guidance for the comparative evaluation and refinement of AmpSeq panels.



124 **Figure 1. Amplicon sequencing and other genotyping approaches for genomic epidemiology of**
125 **infectious diseases.**

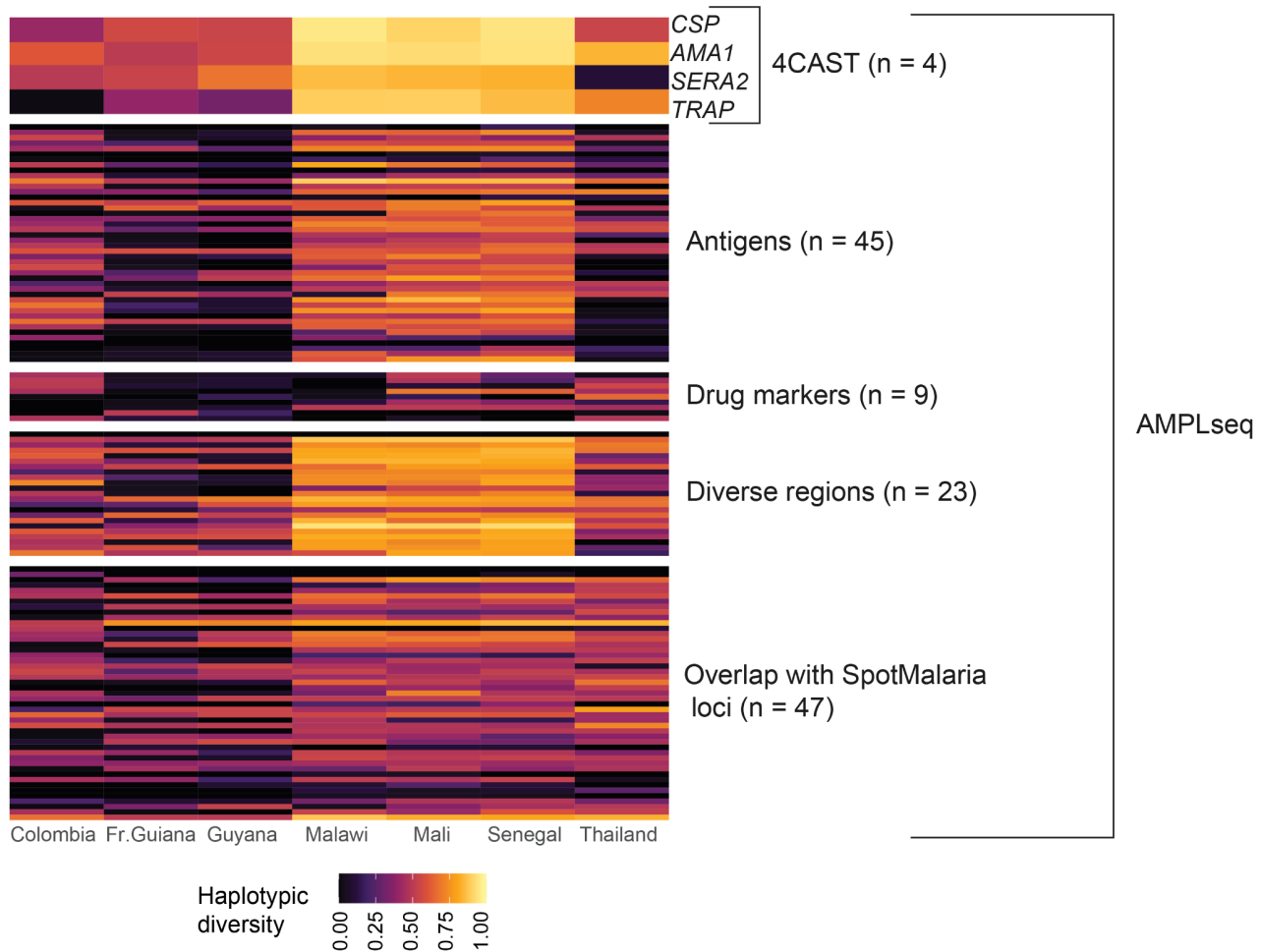
126 Schematic of three common approaches for molecular surveillance data generation. Genomic DNA can
127 be extracted from clinical samples and then processed using any of the three methods shown: SNP
128 barcoding, amplicon sequencing, or whole genome sequencing (WGS). Our two amplicon panels,
129 AMPLseq and 4CAST, are shown, with representations of their loci and amplification. Pre-amplification
130 (selective whole genome amplification), which increases the ratio of parasite to human DNA in samples,
131 is generally recommended for WGS and some amplicon sequencing panels (AMPLseq, but not 4CAST).
132 SNP barcoding provides data in the form of variant calls at each SNP; amplicon sequencing provides
133 extremely deep coverage at select, small regions of the genome; and WGS generally provides shallower
134 coverage of the entire genome.

135 **Materials and Methods**

136 Panel designs

137 We developed a small multiplex of four highly polymorphic antigenic loci, dubbed '4CAST': *CSP*,
138 *AMA1*, *SERA2*, and *TRAP* (**Fig. 2**). All four amplicons use previously published primer sequences (Miller
139 et al., 2017; Neafsey et al., 2015), as no modification was required for successful multiplexing.

140 In designing the larger 'AMPLseq' multiplexed amplicon panel, we first built a large pool of
141 candidate loci, anticipating significant attrition of candidates due to primer incompatibility. We prioritized
142 four classes of loci: loci within antigens of interest (Helb et al., 2015), loci with high population diversity
143 for relatedness inference (Taylor et al., 2019), loci included in the SpotMalaria v1 panel (Chang et al.,
144 2019; Jacob et al., 2021), and known drug resistance markers. We contracted the services of GTseek
145 LLC (<https://gtseek.com>) to design multiplexed oligo panels according to the criteria previously described
146 for the Genotyping-in-Thousands by sequencing (GT-seq) protocol (Campbell, Harmon, & Narum, 2015)
147 (**S1 Supporting information**). We optimized the final primer set and reaction conditions through
148 several sequencing runs and determined that the primers for the four 4CAST loci (*CSP*, *AMA1*, *SERA2*,
149 *TRAP*) could be added to the panel without impacting amplification of the other loci. We also successfully
150 added primers amplifying known markers of antimalarial drug resistance within the genes *dhfr*, *dhps*,
151 *mdr1*, and *kelch13* (**S2 Table**). Furthermore, we successfully added previously described primers for
152 *PvDHFR* (Lefterova, Budvytiene, Sandlund, Färnert, & Banaei, 2015) in order to identify *P. falciparum* / *P.*
153 *vivax* co-infections that have gone undetected in preliminary screening by microscopy or rapid diagnostic
154 test (RDT). The final panel, dubbed 'AMPLseq' (short for Assorted Mix of *Plasmodium* Loci) contains this
155 single *P. vivax* locus and 128 *P. falciparum* loci (**Fig. 2**), with a median length across all amplicons of 276
156 bp (**S1 Fig.**).



157 **Figure 2. Global characterization of loci in the 4CAST and AMPLseq panels.**

158 Estimates of diversity of each locus in the 4CAST and AMPLseq panels, with one locus per row. We
159 estimated haplotypic diversity from monoclonal *P. falciparum* WGS data from each country. The top 4 loci
160 shown represent the 4CAST loci, which are also included in the AMPLseq panel. All 128 *P. falciparum*
161 loci in the AMPLseq panel are shown; the single *P. vivax* locus is not shown.

162 **Panel protocols**

163 To create the primer pool used in 4CAST PCR1, we combined 100 μM of each 4CAST primer (**S3**
164 **Table**) and diluted the combined primer mix to 6.25 μM per primer in nuclease-free water (NF dH₂O).

165 Each 10.5 μl PCR1 reaction incorporated 1.5 μl combined primer mix, 5 μl KAPA HiFi HotStart ReadyMix
166 (2x), and 4 μl sample template. PCR1 amplification consisted of an initial incubation step at 95 $^{\circ}\text{C}$ (3

167 min); 25 amplification cycles at 95 $^{\circ}\text{C}$ (20 s), 57 $^{\circ}\text{C}$ (15 s) and 62 $^{\circ}\text{C}$ (30 s); and a final extension step at

168 72 $^{\circ}\text{C}$ (1 min). Each 12.2 μl PCR2 reaction (which adds sample indices and sequencing adapters)

169 incorporated 2.2 μl unique dual index (10 μM Illumina Nextera DNA UD Indexes), 5 μl KAPA HiFi

170 HotStart ReadyMix (2x), 2 μl NF dH₂O and 3 μl PCR1 product. PCR2 consisted of an initial incubation

171 step at 95 °C (1 min); 10 amplification cycles at 95 °C (15 s), 55 °C (15 s) and 72 °C (30 s); and a final
172 extension step at 72 °C (1 min). We combined PCR2 products in equal volumes and performed
173 double-sided size selection using Agencourt AMPure XP beads (Beckman Coulter): we incubated 100 µl
174 library with 55 µl beads, immobilized beads via magnet rack, and transferred the supernatant to a new
175 tube. We incubated the transferred supernatant with 20 µl beads and washed immobilized beads twice
176 with 80% ethanol. We eluted the library in 25 µl EB buffer (10 mM Tris-Cl, pH 8.5), subsequently adding
177 2.5 µl EB buffer with 1% Tween-20. We verified size selection via Agilent BioAnalyzer 2100 and
178 sequenced the selected library at 6 pM with >10% PhiX in paired-end, 500-cycle format using MiSeq
179 Reagent Kit v2 (**S1 Protocol**).

180 We followed a similar nested PCR and pooled clean-up procedure for AMPLseq library
181 construction. Primer sequences, input volumes and concentrations are listed in **S3 Table** and PCR
182 conditions and size selection steps are shown in **S2 Protocol**. As detailed therein, library construction for
183 AMPLseq library construction differs in a few minor aspects. For example, primer input quantities vary
184 slightly (800 pmol +/- 33%) to account for amplification rate differences among loci. PCR1 products are
185 diluted 1:12 in NF dH₂O prior to PCR2 and only single-sided (left-tailed) bead-based size selection is
186 used to enhance yield. Sequencing also occurs via paired-end, 500-cycle MiSeq but with a higher final
187 library loading concentration (12 pM) and a lower fraction of PhiX (8%).

188 **Mock samples**

189 We generated mock samples from parasite lines 3D7 and Dd2, cultured at 3% hematocrit in
190 commercially obtained red blood cells as previously described (Trager & Jensen, 1976). We extracted
191 genomic DNA using the Qiagen Blood and Tissue Kit on cells previously lysed with 0.15% saponin. We
192 generated positive control template representing DNA extractions from whole human blood infected with
193 10,000 monoclonal 3D7 parasites/µl by diluting genomic DNA from 3D7 to 0.25 ng/µl in 10 ng/µl human
194 genomic DNA, and storing in 10 mM Tris-HCl (pH 8.0), 1 mM EDTA (Promega, Madison, WI). We
195 generated further control templates representing 1000, 100, and 10 3D7 parasites/µl by serial 1:10
196 dilution of the 10,000 3D7 parasites/µl control, likewise using 10 ng/µl human genomic DNA as diluent.

197 We also generated a 10,000 parasites/ μ l positive control as described above but using Dd2 instead of
198 3D7 strain genomic DNA. We generated mixed-strain control templates by combining the 10,000 3D7
199 parasites/ μ l control with this 10,000 Dd2 parasites/ μ l control at 1:1, 3:1, and 10:1 ratios (respectively).
200 We serially diluted the 1:1 ratio to 1000, 100, and 10 parasites/ μ l concentrations and diluted the 3:1 and
201 10:1 ratios to 1000 and 100 parasites/ μ l concentrations using 10 ng/ μ l human genomic DNA diluent as
202 before. We also applied selective whole genome amplification (sWGA) to all above control templates
203 representing \leq 1000 parasites/ μ l. The 50 μ l sWGA reaction followed Oyola *et al.* 2016 (Oyola et al.,
204 2016) with the exception of fixing template input volume to 10 μ L. We purified sWGA products with
205 Agencourt AMPure XP beads (Beckman Coulter) on the KingFisher Flex (**S3 Protocol**) and verified
206 amplification success via NanoDrop (ThermoFisher Scientific).

207 **Clinical samples**

208 We tested the panels on clinical dried blood spot (DBS) samples from Mali and Guyana. Tran *et*
209 *al.* collected samples in Kalifabougou, Mali in 2011 – 2013 as previously described (Tran et al., 2013).
210 The Kalifabougou cohort study was approved by the Ethics Committee of the Faculty of Medicine,
211 Pharmacy and Dentistry at the University of Sciences, Technique and Technology of Bamako, and the
212 Institutional Review Board of the National Institute of Allergy and Infectious Diseases, National Institutes
213 of Health (NIH IRB protocol number: 11IN126; <https://clinicaltrials.gov/>; trial number NCT01322581).
214 Written informed consent was obtained from participants or parents or guardians of participating children
215 before inclusion in the study. The Guyana Ministry of Health collected samples from Port Kaituma and
216 Georgetown, Guyana between May – August 2020, by spotting participants' whole blood onto Whatman
217 FTA cards and storing the samples with individual desiccant packets at room temperature. Informed
218 consent (or parental assent for minors) was obtained for all subjects according to protocols approved by
219 ethical committees.

220 We punched DBS samples 3 – 5 times into a 96-well deep well plate using the DBS pneumatic
221 card puncher (Analytical Sales and Services, Inc.) equipped with a 3 mm cutter. We then extracted gDNA
222 following the DNA purification from buccal swab section of the KingFisher Ready DNA Ultra 2.0 Prefilled

223 Plates for KingFisher Flex instruments protocol (ThermoFisher Scientific) with minor modifications (**S4**
224 **Protocol**). We used the same sWGA procedure as above on the extracted gDNA.

225 **Whole genome sequencing and variant calling**

226 We performed whole genome sequencing on clinical samples collected in Guyana to validate
227 4CAST and AMPLseq outcomes. We performed sWGA on DNA samples as described above to enrich
228 parasite DNA. We used the enriched DNA to construct Illumina sequencing libraries from the amplified
229 material using the NEBNext Ultra II FS DNA prep kit (NEB #E6177) prior to sequencing on an Illumina
230 HiSeqX instrument at the Broad Institute, using 150 bp paired-end reads, targeting a sequencing depth
231 of at least 50X coverage. We aligned reads to the *P. falciparum* v3 reference genome assembly using
232 BWA-MEM (Li, 2013) and called SNPs and INDELS using the GATK HaplotypeCaller (DePristo et al.,
233 2011; McKenna et al., 2010; Van der Auwera et al., 2013) according to the best practices for *P.*
234 *falciparum* as determined by the Pf3k consortium (<https://www.malariagen.net/resource/34>). Analyses
235 were limited to the callable segments of the genome (Miles et al., 2016) and excluded sites where over
236 20% of samples were multiallelic. Data from these samples were submitted to the NCBI Sequence Read
237 Archive (<http://www.ncbi.nlm.nih.gov/sra>) under accession PRJNA758191.

238 **Amplicon data analysis**

239 We developed an application named AmpSeQC (**S2 Supporting information**) to assess
240 sequence quality and amplicon/sequence run success (**S2 Fig.**). We also used AmpSeQC for *P. vivax*
241 detection by applying a concatenation of the *P. falciparum* 3D7 and *P. vivax* PvP01 reference genomes
242 during the BWA-MEM alignment step. For in-depth assessment of *P. falciparum* sequence variation, we
243 processed paired-end Illumina sequencing data in the form of FASTQ files using a custom analysis
244 pipeline (**S2 Supporting information**) that leverages the Divisive Amplicon Denoising Algorithm
245 (DADA2) tool designed by Callahan *et al.* 2016 (Callahan et al., 2016) to obtain microhaplotypes (**S2**
246 **Fig.**). We mapped microhaplotypes obtained from DADA2 against a custom-built database of 3D7 and
247 Dd2 reference sequences for each amplicon locus and filtered microhaplotypes based on edit distance,

248 length, and chimeric identification, using a custom R script. (**S2 Supporting information**). We
249 summarized observed sequence polymorphism into a concise format by converting individual
250 microhaplotypes into pseudo-CIGAR strings using a custom python script. Microhaplotypes were
251 discarded if supported by fewer than 10 read-pairs or by less than 1% total read-pairs within the locus, or
252 if they exhibited other error features (**S3 Supporting information**).

253 We analyzed native and pre-amplified mock samples to determine precision and sensitivity of the
254 DADA2 pipeline and filters. We defined a true positive (TP) as a microhaplotype with a pseudo-CIGAR
255 string identical to the reference strain (either 3D7 or Dd2). We defined a false positive (FP) as a
256 microhaplotype with a pseudo-CIGAR string not matching 3D7 (in the case of samples containing only
257 3D7) or not matching 3D7 or Dd2 (in the case of the mixes), and we defined a false negative (FN) as a
258 locus without any correct microhaplotype representation. We defined precision as $TP/(TP+FP)$, and
259 sensitivity (recall) as $TP/(TP+FN)$. Forty-two of 128 *P. falciparum* loci in AMPLseq exhibit identical 3D7
260 and Dd2 reference sequences; we only included these in precision and sensitivity calculations for pure
261 3D7 controls (*i.e.*, $TP+FN = 128$); precision and sensitivity calculations for strain mixtures considered
262 only the 86 loci that differ between 3D7 and Dd2 reference sequences (*i.e.*, $TP+FN = 86$).

263 All amplicon sequencing data were submitted to the NCBI Sequence Read Archive
264 (<http://www.ncbi.nlm.nih.gov/sra>) under accession PRJNA758191.

265 **Comparator Panels**

266 We compared AMPLseq and 4CAST to two previously published AmpSeq panels for malaria
267 molecular surveillance, Paragon HeOME v1 (Tessema et al., 2020) and SpotMalaria v2 (Jacob et al.,
268 2021).

269 Paragon HeOME v1, designed via CleanPlex algorithm (Paragon Genomics Inc, USA), contains
270 100 primer pairs in a single pool. These target 89 *P. falciparum* loci selected based on high diversity and
271 differentiation ($Jost D \geq 0.21$) among clinical isolates from Africa as well as eleven drug
272 resistance-associated loci. A distinctive feature of HeOME library construction involves its requirement

273 for bead-based clean-up and CleanPlex digestion of each sample between PCR1 and PCR2. The
274 protocol therefore does not require sWGA prior to PCR1.

275 SpotMalaria v2, designed via Agena BioScience and MPrimer design software, contains 136
276 primer pairs divided into three different pools. These target loci were considered best able to recapitulate
277 pairwise genetic distance, population differentiation, and sample heterozygosity inferences from global
278 WGS data (MalariaGEN *Plasmodium falciparum* Community Project, 2016). Primers also target various
279 drug resistance-associated loci (some known to exhibit copy number variation) and mitochondrial loci
280 with conserved primer binding sites among *Plasmodium* spp. Library construction requires sWGA prior to
281 PCR1 but no special processing between PCR1 and PCR2.

282 We also compared our amplicon panels to a 24-SNP molecular barcode assay (Daniels et al.,
283 2008). The SNPs targeted by this Taqman qPCR-based assay were chosen principally for their high
284 minor allele frequency (average MAF > 0.35) in parasite sample collections from Thailand and Senegal
285 (Daniels et al., 2008).

286 **paneljudge and *in silico* data simulations**

287 We used WGS data to simulate genotypic panel data for simulations. This publication uses data
288 from the MalariaGEN *Plasmodium falciparum* Community Project as described online pending
289 publication and public release of dataset Pf7 (<https://www.malariagen.net/resource/34>). Specifically, we
290 used genomic data from monoclonal samples collected in Mali, Malawi, Senegal, and Thailand (Zhu et
291 al., 2019), and from Colombia and Venezuela (ENA accession numbers in **S4 Table**). We also used
292 previously published monoclonal genomic data from Guyana (SRA BioProject PRJNA543530) (Mathieu
293 et al., 2020) and French Guiana (SRA BioProject PRJNA242182) (Pelleau et al., 2015). We used the
294 *scikit-allele* library (Miles et al., 2020) to process the data and then estimate microhaplotype frequency
295 and diversity. Specifically, we used the `read_vcf`, `is_het`, and `haploidify_samples` functions as described
296 (**S1 Supporting information**), and we estimated haplotype frequencies with the `distinct_frequencies`
297 function.

298 We assessed the performance of different panels for relatedness inference using simulated data.
299 We generated data on pairs of haploid genotypes (equivalent to pairs of monoclonal malaria samples)

300 using paneljudge (Taylor & Jacob, 2020), an R package that we built to simulate data under a hidden
301 Markov model (HMM) (Taylor et al., 2019) (**S2 Supporting information**). For each panel, we calculated
302 inter-locus distances from the median nucleotide position of each locus and set distances as infinite
303 between chromosomes. For each panel and population of interest, we calculated haplotype frequency
304 estimates using *scikit-allele*, as described above. Given these distances and frequency estimates, we
305 simulated data using relatedness parameter values of 0.01 (unrelated), 0.50 (siblings), and 0.99 (clonal),
306 and switch rate parameter values of 1, 5, 10, and 50. For each combination of panel, population,
307 relatedness parameter, and switch rate parameter, we simulated data on 100 haploid genotype pairs. For
308 each haploid genotype pair, we then generated estimates of the relatedness parameter and the switch
309 rate parameter using paneljudge, with 95% confidence intervals (CIs), under the same model used to
310 simulate the data. We next performed relationship classification from these estimates and CIs. For
311 estimates of unrelated pairs (relatedness parameter of 0.01), we generously classified estimates as
312 correct if the lower limit of the 95% confidence interval (LCI) was below or equal to 0.01 and the upper
313 limit of the 95% confidence interval (UCI) was below 0.99. We classified estimates of sibling-level
314 relatedness (0.50) as correct if the LCI was above 0.01 and the UCI was below 0.99. We classified
315 estimates of clonal pairs (0.99) as correct if the LCI was above 0.01 and the UCI was above or equal to
316 0.99. In all relatedness levels, if the 95% confidence interval spanned both 0.01 and 0.99 (*i.e.*, $LCI < 0.01$
317 and $UCI > 0.99$), then we denoted the estimate as unclassified.

318 To evaluate panel performance in COI estimation, we combined monoclonal WGS data to
319 engineer *in silico* polyclonal samples using *vcftools* (Danecek et al., 2011). We then estimated
320 microhaplotype frequencies for each locus of a given panel, using *scikit-allele* as described above, and
321 counted the number of distinct microhaplotypes observed at each locus per sample. We estimated COI
322 as the maximum number of distinct microhaplotypes observed at any locus within a sample.

323 To evaluate panel performance for geographic attribution, we identified microhaplotypes at loci as
324 described above. We used the microhaplotype sequences themselves and visualized these data using
325 the *Rtsne* package (Krijthe, 2015), with 5000 iterations, Θ of 0.0, and perplexity parameters of 10 (for
326 4CAST and the 24 SNP barcode) or 30 (for the remaining panels).

327 **Results**

328 **4CAST and AMPLseq validation**

329 We validated assay precision (defined as $TP/(TP+FP)$), sensitivity (defined as $TP/(TP+FN)$), and
330 depth of coverage using 3D7 mock clinical samples representing parasitemia levels between 10 and
331 10000 parasites/ μ l in 10 ng/ μ l human DNA. Both 4CAST and AMPLseq generated 3D7 microhaplotype
332 calls with 100% precision for all parasitemia levels assessed, both with and without pre-amplification by
333 sWGA. 4CAST achieved high sensitivity and depth without preliminary sWGA, generating a median of 43
334 read-pairs per locus from native templates representing 10 parasites/ μ l (**Fig. 3A**). Median depth
335 increased to 443 and 1312.5 read-pairs per locus for native templates representing 100 and 1000
336 parasites/ μ l, respectively. Read-pair counts were also evenly distributed among 4CAST loci using native
337 DNA (**Fig. 3A**).

338 Unlike 4CAST, AMPLseq required sWGA for 3D7 mock samples representing ≤ 100 parasites/ μ l
339 (**Fig. 3B**). Following sWGA on mock samples representing 10 parasites/ μ l, the assay generated ≥ 10
340 read-pairs at a median of 126 loci, with a median of 465 read-pairs after excluding loci with fewer than 10
341 reads. Values were statistically similar for pre-amplified samples representing 100 parasites/ μ l and
342 increased to 692 read-pairs for pre-amplified samples representing 1000 parasites/ μ l (**S3 Fig.**).

343 We also validated the sensitivity of 4CAST and AMPLseq for genotyping polyclonal infections by
344 using mock samples containing both 3D7 and Dd2 templates (likewise in 10 ng/ μ l human DNA). These
345 mixtures featured Dd2 at 50% (*i.e.*, 1:1 3D7:Dd2 ratio), 25% (3:1), and 9% (10:1) relative abundance.
346 Total parasitemia levels ranged between 10 and 10000 parasites/ μ l. Both 4CAST and AMPLseq
347 generated microhaplotype calls with 100% precision at the 86 loci that are dimorphic between the 3D7
348 and Dd2 references (including all four 4CAST loci and an additional 82 loci in AMPLseq). This perfect
349 precision was observed at all parasitemia levels in both native and pre-amplified mock mixtures of the
350 two strains.

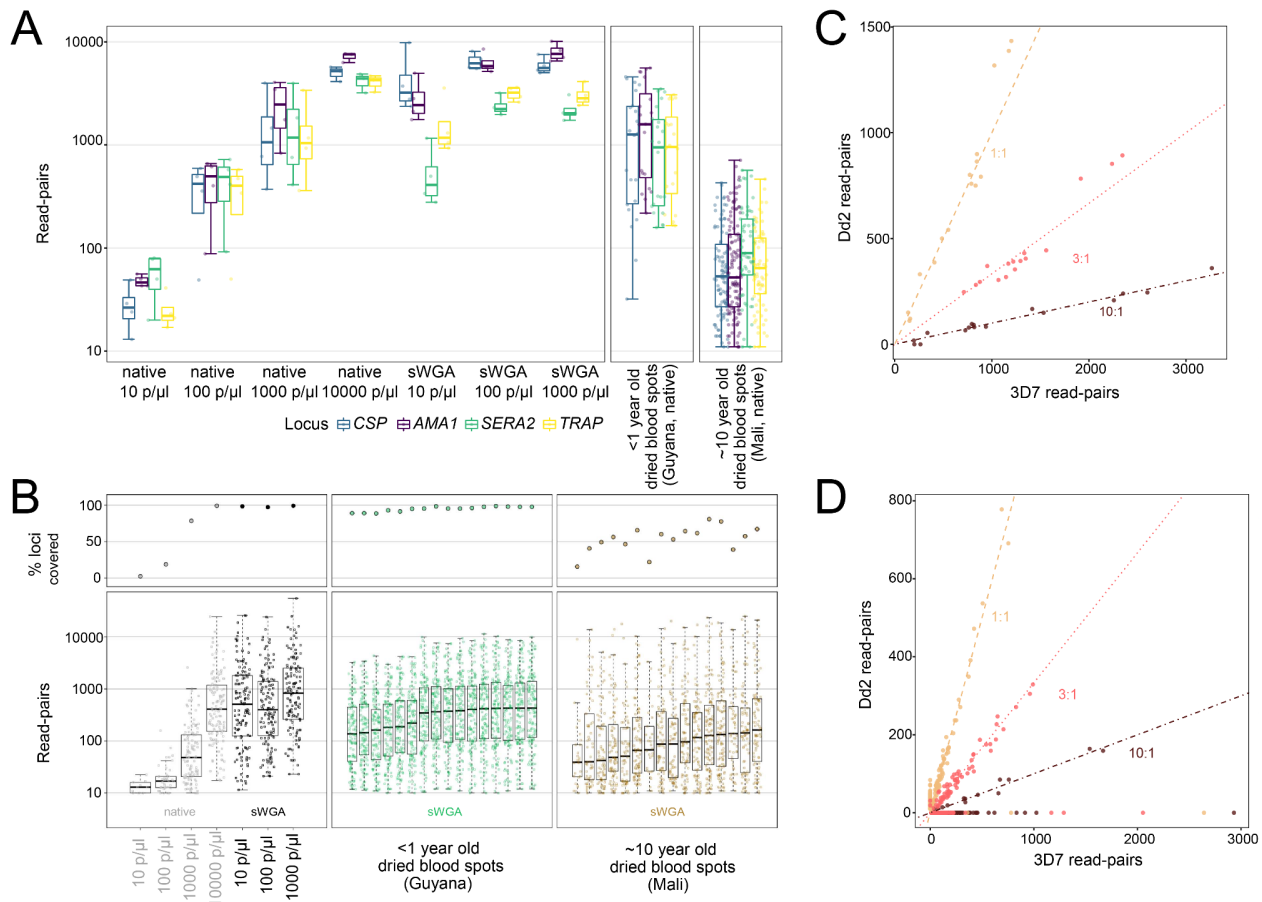
351 4CAST showed high sensitivity for Dd2 without the need for sWGA. At 1000 parasites/ μ l, the
352 assay detected Dd2-specific microhaplotypes at each of its four loci in all 1:1, 3:1, and 10:1 mixture
353 replicates (**Fig. 3C**). At 100 parasites/ μ l, median Dd2 sensitivity remained 100% at 1:1 and 3:1 ratios but

354 lowered slightly to 94% at 10:1. Sensitivity for each strain decreased at 10 parasites/ μ l, with 1:1 ratios
355 yielding a median of 3 target loci for 3D7 and a median of 2 targets for Dd2; median sensitivity in these
356 samples rose to 3.5 and 3 loci (respectively) following pre-amplification with sWGA, but this led to
357 unbalanced read-pair support between the two strains (**S4A Fig.**), possibly due to differential sWGA
358 success on low-quality Dd2 vs. high-quality 3D7 templates. 4CAST read-pair ratios generated from
359 native templates, by contrast, showed a very high correlation with input ratios at 100 p/ μ l (**S4A Fig.**) and
360 1000 p/ μ l (**Fig. 3C**). Ratios became less informative at 10 parasites/ μ l (**S4A Fig.**).

361 AMPLseq (with sWGA) was also successful in detecting Dd2-specific microhaplotypes, but only
362 at a maximum of 77 of 86 dimorphic loci (in the 1:1 ratio at 10000 parasites/ μ l). Dd2-specific sequences
363 were detected at a minimum of two dimorphic loci for all three input ratios (1:1, 3:1, 10:1) and
364 parasitemia levels (≥ 10 p/ μ l) assessed. Like with 4CAST, however, the use of sWGA decorrelated
365 read-pair ratios from input ratios (**S4B Fig.**). Dd2 sensitivity was also reduced relative to 3D7 sensitivity
366 (median Dd2 sensitivity / 3D7 sensitivity = 58%) with sWGA. These discrepancies were not observed
367 with native templates (**Fig. 3D**) at ≥ 1000 parasites/ μ l for which AMPLseq achieves high read-pair support
368 without the use of sWGA.

369 We also tested both panels on genomic DNA extracted from dried blood spots collected by the
370 Guyana Ministry of Health in 2020 from individuals diagnosed as *P. falciparum*-positive via a rapid
371 diagnostic test (RDT). Ten Guyanese samples were tested with both panels, and an additional six were
372 tested with AMPLseq. Using 4CAST, we observed coverage across all loci in all samples, with a median
373 read-pair depth per locus of 1162 read-pairs without sWGA (**Fig. 3A**). Using AMPLseq (with sWGA), we
374 observed a median of 122 loci with ≥ 10 read-pairs and a median read-pair depth of 298 read-pairs per
375 covered locus (**Fig. 3B**).

376 Additionally, we tested both panels on gDNA extracted from 16 dried blood spot samples
377 collected in Mali in 2011 (Tran et al., 2013) and subsequently stored at room temperature for ten years.
378 Using 4CAST (without sWGA), we observed a median read-depth of 407 read-pairs per locus (**Fig. 3A**).
379 Using AMPLseq (with sWGA), we observed a median of 75 loci with ≥ 10 read-pairs and a median
380 read-depth of 112 read-pairs per covered locus (**Fig. 3B**).



381 **Figure 3. 4CAST and AMPLseq panel validation with mock and clinical samples.**

382 A) Boxplots of read-pairs per locus in the 4CAST panel. The first facet shows read-depth per locus
 383 across mock samples ranging from 10 - 10000 p/μl, both native DNA and sWGA DNA (n=4 per
 384 condition). The second and third facets show read-depth per locus across two sets of clinical samples,
 385 <1 year old and ~10 year old dried blood spots, respectively (n=32 per sample set). B) The same 3D7
 386 mock sample sets were used to assess AMPLseq sensitivity (top left panel of B) and sequencing depth
 387 (bottom left panel of B). Each point in the bottom left panel of B represents read-pair support for one
 388 AMPLseq locus. Positions on the y-axis indicate median read-pair support across replicate samples. Low
 389 sensitivity observed using native templates (grey) representing ≤ 100 3D7 parasites/μl suggests that
 390 clinical samples should be pre-amplified with sWGA (results at right). C) Ratio of read-pairs from
 391 microhaplotypes assigned to 3D7 (x-axis) or Dd2 (y-axis) from mock mixtures of these DNAs in ratios of
 392 1:1 (tan), 3:1 (pink), and 10:1 (dark red). All samples contained 1000 parasites per μl total, across both
 393 DNA sources. Dashed lines represent the expected ratio, and each point represents a 4CAST locus per
 394 sample (n=4 per condition). D) AMPLseq read-pair ratios observed in native 3D7+Dd2 mock mixtures
 395 (1000 parasites/μl) are plotted as above (C) for 4CAST.

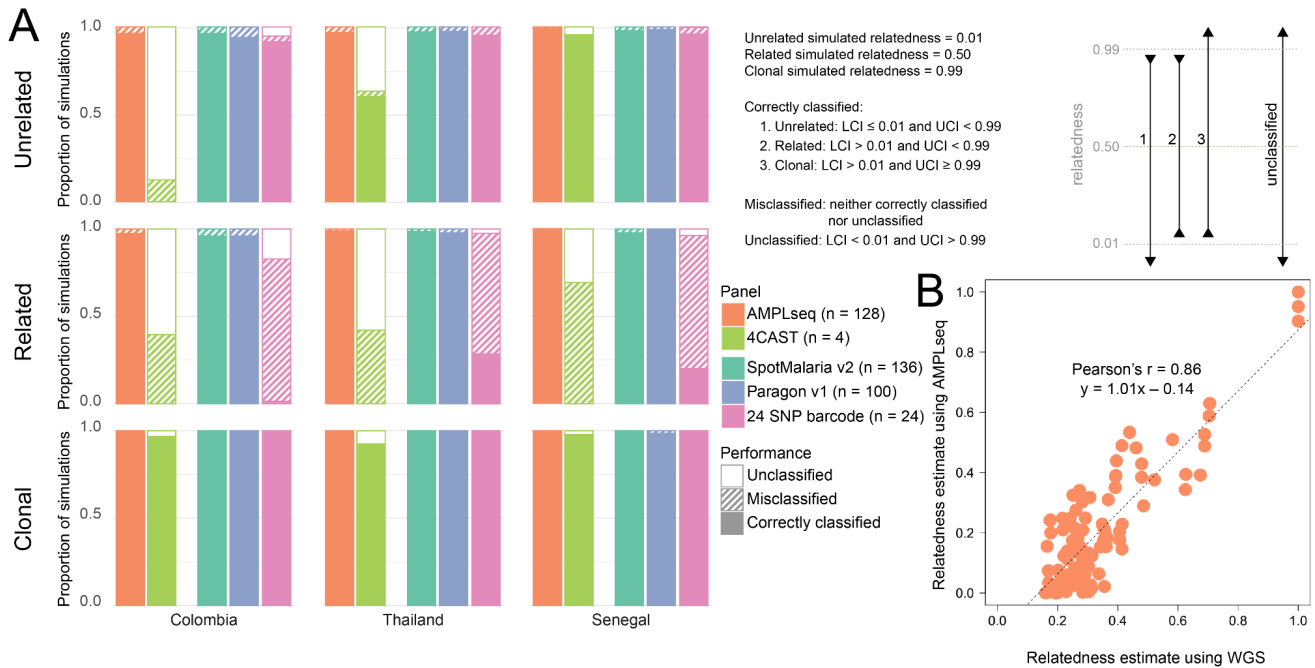
396 Evaluation of panel performance for relatedness

397 We used the R package paneljudge to assess *in silico* the impact of choosing a specific
 398 genotyping panel for relatedness inference. Considering the choice of panel, we evaluated relatedness

399 estimation from data simulated on our 4CAST and AMPLseq panels, the SpotMalaria v2 (Jacob et al.,
400 2021) and Paragon HeOME v1 (Tessema et al., 2020) amplicon panels, and a barcode of 24 SNPs.
401 When data were simulated using microhaplotype frequency estimates of Senegalese parasites, we found
402 that almost all estimates of unrelated or clonal pairs were correctly classified, regardless of the panel
403 (**Fig. 4A**). All three large panels also performed similarly well in accurately identifying partially-related
404 parasite pairs, despite being the product of three distinct design processes. Neither 4CAST nor the 24
405 SNP barcode estimated relatedness for partially-related samples as well as the larger panels. We also
406 evaluated panel performance in less diverse parasite populations (Colombia and Thailand), including a
407 population not used in the panel designs (Colombia). We repeated the simulations using microhaplotype
408 frequencies estimated with these data. Again, we found that all panels performed well for estimating
409 relatedness of clonal pairs, and that the 24 SNP barcode and 4CAST were less likely to have correctly
410 classified estimates of non-clonal pairs. With the data simulated using Colombian microhaplotype
411 frequencies from the Pacific Coast region, all three large panels performed well for all three relatedness
412 values, despite the Colombian data not having informed the design of any of the panels.

413 Pairwise relatedness estimates (Schaffner et al., 2018) from AMPLseq correlated highly with
414 those from WGS data available for the Guyanese sample set (Pearson's $r = 0.86$, slope = 1.01, $p <$
415 0.001) (**Fig. 4B**). Despite patient travel history metadata suggesting infections to have occurred in
416 various geographic regions of Guyana (**S1 Table**), AMPLseq relatedness estimates for the Guyanese
417 sample set are significantly higher than those for the Malian sample set (Mann Whitney U, $p < 0.001$),
418 consistent with anticipated lower transmission levels in Guyana. Nevertheless, the wide range of
419 relatedness estimates (0.007 – 1) observed among Guyanese sample comparisons suggests AMPLseq
420 capacity to indicate epidemiologically relevant microstructure even in relatively unstructured parasite
421 populations. For example, the first (lowest) quartile of pairwise relatedness estimates from Guyana was
422 enriched for comparisons involving A2-GUY and C5-GUY, two highly related samples that in whole
423 genome analysis show 50% relatedness with a sample from Venezuela (SPT26229, see **S4 Table**).

It is made available under a [CC-BY-NC-ND 4.0 International license](https://creativecommons.org/licenses/by-nc-nd/4.0/).



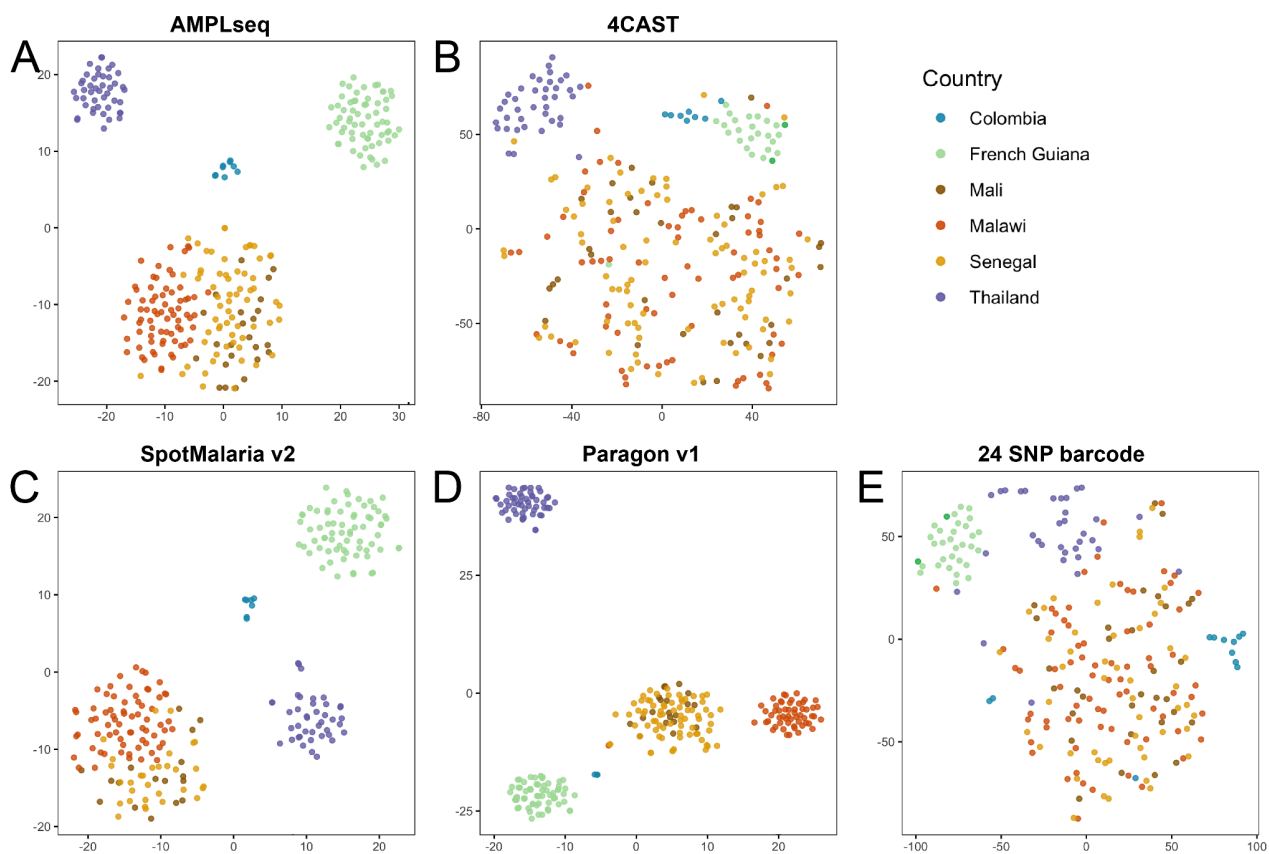
424 **Figure 4. *In silico* relatedness estimation comparisons among panels and empirical AMPLseq**
 425 **validation against WGS.**

426 A) Evaluation of relatedness estimation from data simulated on genotyping panels using the paneljudge
 427 R package. Pairs of haploid genotypes were simulated at each locus of a panel, using microhaplotype
 428 frequencies estimated from a given parasite population (Colombia, Thailand, or Senegal, as shown in
 429 columns from left to right). Genotype pairs were simulated at three levels of relatedness: unrelated
 430 (relatedness = 0.01), related (relatedness = 0.50), and clonal (relatedness = 0.99), as shown in the rows
 431 from top to bottom. Relatedness estimates of these pairs were classified using their 95% confidence
 432 intervals (LCI = lower limit of the 95% confidence interval, UCI = upper limit of the 95% confidence
 433 interval). Estimates could be correctly classified, misclassified, or unclassified, as described in the grey
 434 box. Each bar represents the proportion of simulations per condition (n = 400) classified in each
 435 category. Bars that are filled with a color represent correctly classified simulations, bars that are hashed
 436 represent misclassified simulations, and bars that are filled with white represent simulations that were
 437 unable to be classified. The colors of the bars represent the panel used in that set of simulations. B)
 438 Empirical AMPLseq results recapitulate WGS-based relatedness inference. Points represent relatedness
 439 estimates (hmmIBD (Schaffner et al., 2018) 'fract_sites_IBD' computed under default settings) for pairs
 440 of Guyanese samples using WGS (n= 9408 variants) vs. AMPLseq (n = 220 variants, from within 128
 441 AMPLseq *P. falciparum* loci).

442 **Geographic attribution**

443 We again engineered amplicon data *in silico* to evaluate the relative signal in genotyping panels
 444 for geographic attribution of samples (**Fig. 5**). By sub-sampling WGS variant calls, calling
 445 microhaplotypes, and visualizing these data using t-SNE plots, we found that results from both the 24
 446 SNP barcode (Daniels et al., 2008) and 4CAST distinguished samples by continent of origin, though not
 447 by country. Results from all three larger panels additionally distinguished non-African samples by

448 country, and these panels separated East African (Malawi) from West African samples (Mali/Senegal) to
449 varying degrees; no panel was able to distinguish between Malian and Senegalese samples in this
450 visualization. We also added empirical AMPLseq data from 5 Guyanese samples (C3-GUY, C4-GUY,
451 C5-GUY, C7-GUY, and C8-GUY) and WGS data sub-sampled to AMPLseq coordinates for Venezuelan
452 sample SPT26229 (**S5 Fig.**). The AMPLseq samples formed a small cluster beside the WGS-based
453 Guyanese and French Guianese samples. The Venezuelan sample SPT26229 also placed on the
454 perimeter of the Guyana/French Guiana sample cluster, sharing the same axis-2 position as the
455 empirical AMPLseq points. Results show that empirical AMPLseq data can distinguish autochthonous
456 samples from the Guiana shield, and we expect geographic attribution in the region to improve as more
457 data are collected from infections originating in Venezuela and other undersampled localities.



458 **Figure 5. *In silico* geographic attribution comparison among panels.**

459 Visualization of WGS data subset to coordinates of genotyping panels. Microhaplotypes called at each
460 locus were visualized using tSNE through the Rtsne package, with parameter Θ of 0.0, 5000 iterations,
461 and a perplexity parameter of 30 (A, C, D) or 10 (B, E). Each dot represents a single sample, colored by
462 its country of origin (which was not included in the tSNE algorithm). One genotyping panel is visualized in
463 each plot: (A) AMPLseq, (B) 4CAST, (C) SpotMalaria v2, (D) Paragon v1, (E) 24 SNP barcode.

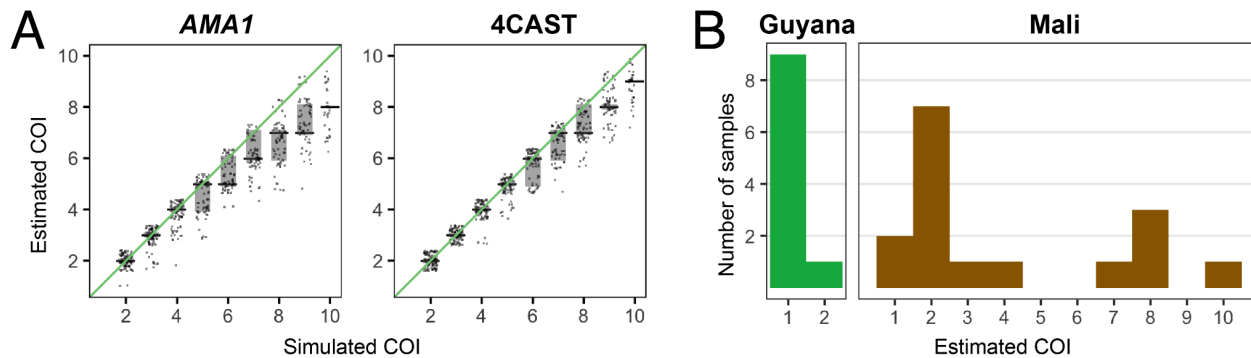
464 **COI estimation**

465 We evaluated COI estimation based on 4CAST as opposed to the single locus *AMA1*, which is
466 commonly used for this purpose, alone or with another locus (Lerch et al., 2017; Miller et al., 2017;
467 Nelson et al., 2019). We engineered *in silico* samples with COI ranging from 2 – 10 (100 simulations per
468 COI level) and used the maximum number of unique microhaplotypes present at any locus as a simple
469 objective method to estimate COI. 4CAST provided more accurate estimates of COI than *AMA1* alone in
470 these simulated data, especially at simulated COI levels between 5 and 7. (Fig. 6A). S6 Fig. indicates
471 that estimation improves at simulated COI=8 using AMPLseq, but to reap the full benefit of the larger
472 panel in practice will require a more elaborate probabilistic algorithm that accounts for variable
473 coverage/sensitivity among loci and incorporates a multinomial approach for polyallelic loci.

474 In the absence of such an algorithm, we proceeded with the naive estimation method above to
475 classify COI in the Mali and Guyana clinical samples. Only a single polyclonal infection (C6-GUY)
476 occurred among Guyanese samples assayed by 4CAST. The repeated detection of two *CSP* and *SERA2*
477 alternate alleles at depths ranging from 32 to 168 read-pairs enabled unambiguous COI=2 classification
478 for the sample. WGS sequencing coverage, by contrast, detected only moderately elevated SNP
479 heterozygosity (1.9%) in C6-GUY and this elevation was not sufficient to classify COI>1 via The Real
480 McCoil (Chang et al., 2017) (**S7 Fig.**). AMPLseq also identified COI=2 for C6-GUY but without consistent
481 support between replicates (2 vs. 6 biallelic loci). Six additional Guyanese samples were assayed by
482 AMPLseq and one was classified as COI=2. This sample (A5-GUY) gave a stronger minor variant signal
483 in both AMPLseq (15 biallelic loci in both replicates) and WGS data (10.9% SNP heterozygosity) (**S7**
484 **Fig.**).

485 For the Malian sample set, 4CAST and AMPLseq both classified samples E5-PST030 and
486 C6-PST063 as monoclonal and all other samples as polyclonal based on presence/absence of
487 multiallelic loci. While 4CAST detected as many as 10 alternate alleles (median = 3) per sample locus
488 (**Fig. 6B**), AMPLseq detected at most 4 (median = 2). These results reaffirm 4CAST as a tool of choice
489 for resolving higher COI levels and when parasitemia levels are low. AMPLseq may reach simulated

490 performance levels (**S6 Fig.**) by reducing sample multiplexing or sequencing on higher output platforms
491 (e.g., NovaSeq) for sample sets with low parasitemia.

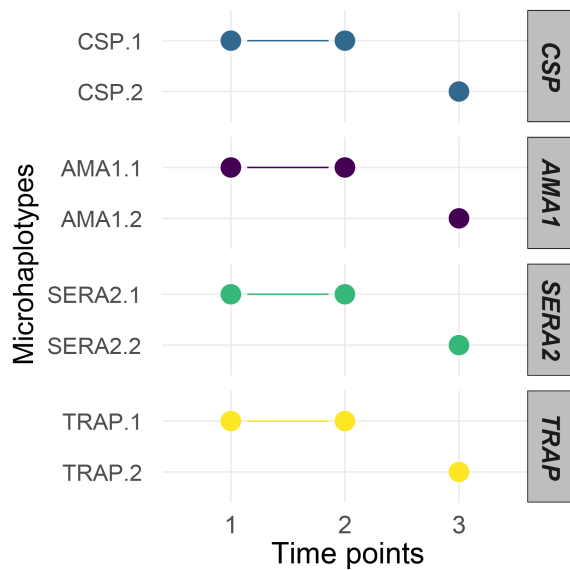


492 **Figure 6. *In silico* and empirical complexity of infection (COI) inference.**

493 A) Scatter plots of estimated COI for samples simulated from combinations of monoclonal WGS data,
494 subsetting to the loci of interest (*AMA1* locus or 4CAST loci). The x-axis represents the number of
495 monoclonal genomes combined into each simulation, and the y-axis represents the COI estimated using
496 the simulated data. COI was naively estimated as the maximum number of unique microhaplotypes
497 present at any locus per sample ($n=100$ samples per condition). Each dot represents a sample, jittered
498 for visibility. The black bars represent the median and light grey boxes represent the 25th – 75th
499 quantiles. B) Estimated COI for clinical samples sequenced using 4CAST. COI was again estimated as
500 the maximum number of unique microhaplotypes present at any locus in the sample.

501 **Longitudinal sampling: distinguishing recrudescence vs. reinfection**

502 We used 4CAST to examine longitudinal samples that were likely to be diverse and polyclonal.
503 We sequenced samples from the same asymptomatic individual in the longitudinal Mali cohort over three
504 consecutive visits (**Fig. 7**) (Tran et al., 2013). We detected a single microhaplotype at each locus that
505 was present in the first two time points, suggesting a continued infection during the two weeks between
506 samples. At the third time point, we detected a single, distinct microhaplotype at each locus, suggesting
507 that a new infection had occurred and the original infection had disappeared or decreased below our limit
508 of detection (<10 p/ μ l). In this particular case, the individual was asymptomatic and did not receive
509 anti-malarial treatment between any samples; however, this simple example demonstrates the clarity that
510 4CAST can bring to tracking infection turnover in longitudinal studies, and suggests its utility in
511 distinguishing recrudescence vs. reinfection in therapeutic efficacy studies.



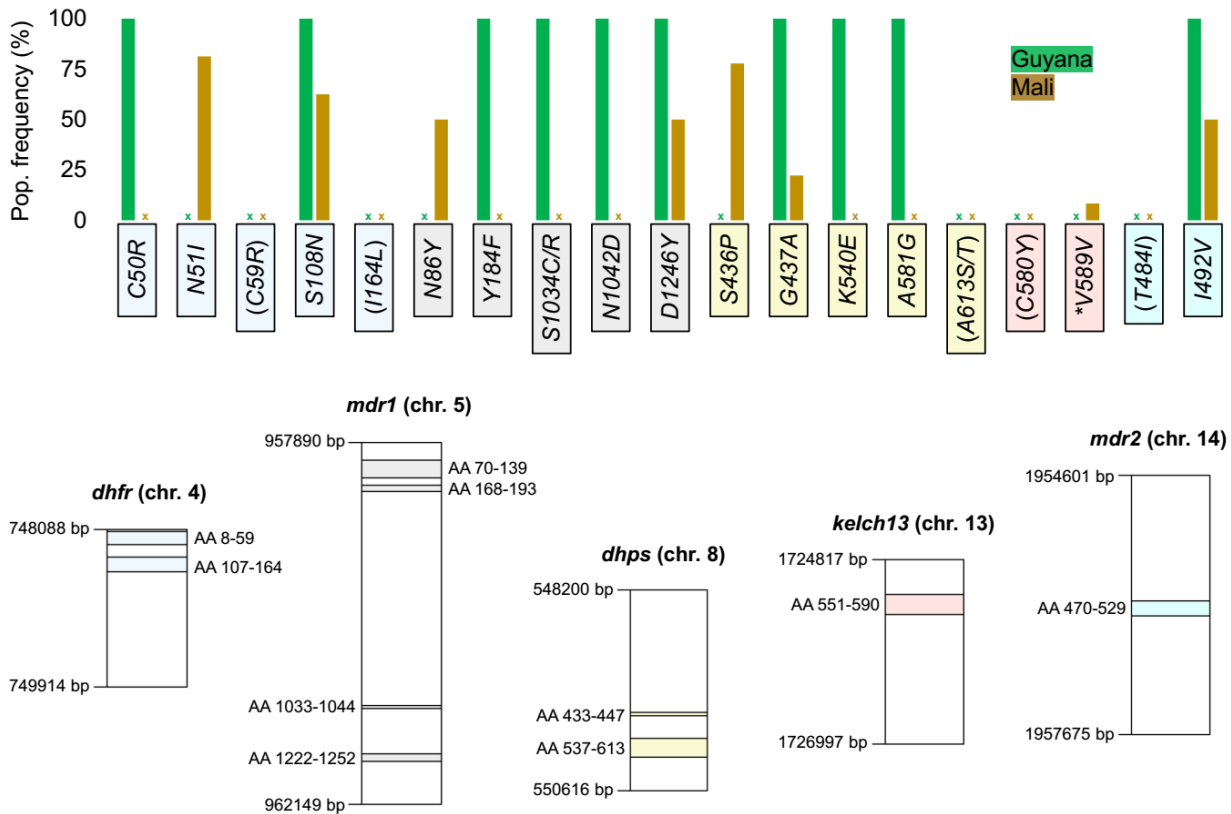
512 **Figure 7. Longitudinal tracking of infections using 4CAST.**

513 Identification of distinct microhaplotypes present in samples from an individual at three consecutive time
514 points. The x-axis represents the three time points, and the y-axis represents the individual
515 microhaplotypes identified, grouped by locus. Dots represent the presence of that microhaplotype,
516 connected when present in consecutive visits.

517 **Drug resistance profiling**

518 *AMPLseq* loci in *dhfr*, *mdr1*, *dhps*, *kelch13*, and *mdr2* contain ten sequence regions that code for
519 various amino acid (AA) polymorphisms that have previously been associated with resistance to
520 antimalarial drugs (Ariey et al., 2014; Miotto et al., 2015; Mita et al., 2007; Veiga et al., 2016)Thirteen of
521 these 18 positions of interest contained nonsynonymous mutations in Malian and Guyanese clinical
522 samples of this study (Fig. 8). Positions of interest that lacked mutations across both sample sets were
523 DHFR AA 59 and 164; DHPS AA 613; KELCH13 AA 580; and MDR2 AA 484. All Guyanese sequences
524 shared the same mutant alleles at many loci. Malian samples, by contrast, did not show fixed mutant
525 alleles at any amino acid position of interest. A mix of mutant and wildtype alleles occurred among
526 Malian samples for DHFR AA 51 and 108; MDR1 AA 86, 184, and 1246; DHPS AA 436 and 437; and
527 MDR2 AA 492. A previously reported synonymous polymorphism was observed in one Malian sample at
528 KELCH13 AA 589 (Taylor et al., 2015).

It is made available under a [CC-BY-NC-ND 4.0 International license](https://creativecommons.org/licenses/by-nc-nd/4.0/).



529 **Figure 8. Drug resistance-associated sequence profiling in Guyanese and Malian clinical**
 530 **samples.**

531 Bars in the top plot indicate the occurrence of various drug resistance-associated amino acid changes
 532 within AMPLseq loci. Positions of interest assayed by AMPLseq but without mutant alleles (see x-marks)
 533 in the clinical samples profiled here are labeled in parentheses. Positions 484 and 492 in *mdr2* have
 534 been suggested to be involved in artemisinin resistance despite lack of experimental data showing an
 535 association with a clinical phenotype (Chenet et al., 2017; Miotto et al., 2015). Bottom plot indicates
 536 chromosomal and amino acid (AA) positions of each drug resistance-associated AMPLseq locus.
 537 Asterisk indicates synonymous mutation within *kelch13*.

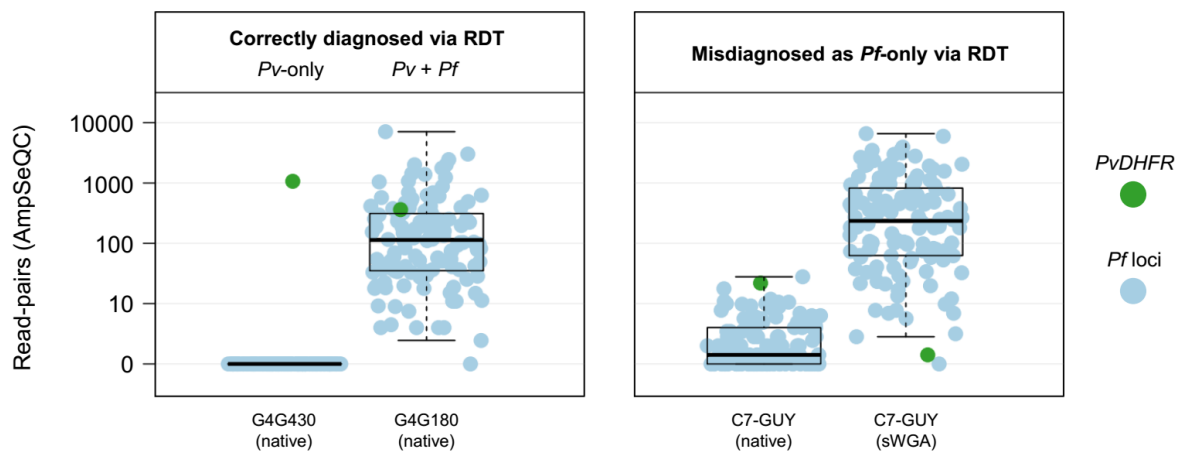
538 *P. falciparum* and *P. vivax* co-infection detection

539 To test the ability of AMPLseq to detect *P. vivax* co-infections via co-amplification of *PvDHFR*, two
 540 additional Guyanese blood spot samples that had been diagnosed as *P. vivax*-only (G4G430) and *P.*
 541 *vivax* + *P. falciparum* co-infection (G4G180) via RDT were included in the sample set. These samples did
 542 not undergo sWGA.

543 *PvDHFR* was detected at high depth in both samples (1068 – 1822 read-pairs for G4G430 and
 544 234 – 560 read-pairs for G4G180) (**Fig. 9**). Only G4G180 also showed read-pair support at *P. falciparum*
 545 panel loci (>10 read-pairs at 100 – 115 loci). *PvDHFR* was not detected in any native or pre-amplified
 546 3D7 or mixed-strain (3D7 + Dd2) templates. This demonstrates high specificity of both *PvDHFR* and *P.*

547 *falciparum* AMPLseq primers to their intended target species without any apparent amplification inhibition
548 by the presence of congeneric DNA.

549 *PvDHFR* was also detected at low levels (16 – 30 read-pairs) in both native template replicates of
550 C7-GUY, one of the sixteen Guyanese samples previously diagnosed as *P. falciparum*-only via RDT.
551 Surprisingly, two *PvDHFR* read-pairs were also detected in one of the two sWGA replicates from the
552 sample, despite the expectation that sWGA would primarily amplify *P. falciparum* sequencines.
553 Sensitivity of *PvDHFR* detection in pre-amplified samples could be enhanced by adding *PvDHFR* primers
554 to the *P. falciparum* sWGA primer pool. *PvDHFR* detection did not occur in any Malian sample,
555 consistent with low prevalence of *P. vivax* in West Africa relative to the Guiana shield.



556 **Figure 9. *Plasmodium vivax* detection by AMPLseq.**

557 The left panel demonstrates strong read support for *PvDHFR* (green circle) in native control samples
558 previously suggested to contain *P. vivax* (*Pv*; G4G430) and *P. vivax* + *P. falciparum* (*Pv* + *Pf*; G4G180)
559 via RDT. The right panel shows native and sWGA results for C7-GUY, a clinical sample that appears to
560 have been misdiagnosed as *Pf*-only prior to AMPLseq. Blue circles represent read support for *P.*
561 *falciparum* loci. Positions on the y-axis indicate median read-pair support across two sample replicates.
562 Box and whiskers indicate quartiles.

563 **Discussion**

564 The utility of AmpSeq for molecular surveillance of infectious diseases is evidenced by the
565 growing number of protocols recently published or under development for *Plasmodium* and other
566 pathogens (Aydemir et al., 2018; Fola et al., 2020; Jacob et al., 2021; Mitchell et al., 2021; Moser et al.,
567 2021; Ruybal-Pesántez et al., 2021; Schwabl et al., 2020; Tessema et al., 2020). Here, we demonstrate

568 the performance of two new panels for *P. falciparum*, designed to serve different use cases and
569 exhibiting different per-sample costs and levels of complexity. Our comparative analyses of these two
570 new panels, AMPLseq and 4CAST, relative to previously published genotyping panels demonstrates that
571 they perform comparably to existing panels of similar composition across use cases, in a diversity of
572 geographic settings, despite different geographic representation in the population genomic data used to
573 inform their designs. This suggests that *de novo* custom panel design may not be required for accurate
574 COI and relatedness estimation in parasite populations from previously unstudied geographic regions.
575 We therefore suggest that future implementation of these panels should be guided by three criteria: 1)
576 the intended use cases for the data, 2) protocol complexity and compatibility with available instruments
577 and expertise, and 3) protocol customizability for locally relevant genetic loci.

578 Considering the first of these criteria, intended use case, our investigations above suggest a
579 straightforward mapping of panels by size and feature to use case. The small 4CAST panel is well suited
580 to COI estimation (**Fig. 6**), and profiles four highly diverse antigens for the same effort and cost
581 traditionally used to profile a single locus. Because of the very high diversity of the loci in the 4CAST
582 panel in most parasite populations, this panel is also well suited to any application requiring genetic
583 delineation of distinct parasite lineages (**Fig. 7**). In therapeutic efficacy studies, for example, it is
584 essential to determine whether subjects who become parasitemic following drug treatment are exhibiting
585 a recrudescence of an incompletely-cleared strain from the initial infection (which could indicate
586 treatment failure), or if they have become reinfected with a distinct parasite strain subsequent to
587 treatment. We suggest that the 4CAST panel would be significantly more informative than traditional
588 genotyping approaches used in therapeutic efficacy studies, such as profiling length polymorphisms or
589 allele-specific amplification in the *MSP1/MSP2/GLURP* loci (Reeder & Marshall, 1994; Snounou, 2002),
590 and more cost-effective than independent monoplex amplification and Illumina sequencing of individual
591 loci (Early et al., 2019; Gruenberg et al., 2019; Lerch et al., 2017).

592 Our work also demonstrates that the AMPLseq panel performs comparably to two existing
593 multiplexed amplicon sequencing panels of similar size (Jacob et al., 2021; Tessema et al., 2020) for any
594 use case reliant on estimation of parasite relatedness (**Fig. 4**), despite different design criteria and

595 datasets that informed the panels. Potential public health use cases that employ relatedness information
596 include measuring the connectivity of parasites between locations to define units of control, and
597 monitoring changes in the level of transmission (Cerqueira et al., 2017; Daniels et al., 2015; Knudson et
598 al., 2020). The AMPLseq panel and its peers are also much better suited to detecting imported infections
599 given their improved capacity to distinguish parasites from distinct geographic locations (**Fig. 5**.) Finally,
600 the larger panels offer the capacity to monitor genetic markers associated with drug resistance (**Fig. 8**)
601 or, in some panels, detect co-infection with other *Plasmodium* species (**Fig. 9**).

602 The second panel selection criterion, protocol complexity and compatibility with available
603 instruments, should be prefaced with a reminder that all of these protocols employ nested PCR reactions
604 as the fundamental mechanism to produce sequencing libraries targeting small genomic regions of
605 interest. Any molecular laboratory with a capacity for PCR and a small sequencing instrument such as an
606 Illumina iSeq100 will be capable of carrying out any of these protocols. The exquisite sensitivity of
607 amplicon sequencing implemented via an Illumina platform means that all of these protocols are also
608 susceptible to contamination. PCR reactions should be conducted in dedicated hoods, ideally in rooms or
609 locations physically removed from settings in which PCR products are manipulated. Finally, all of these
610 protocols share: 1) a requirement for careful cleanup of inappropriately large or small DNA molecules
611 from pooled libraries prior to sequencing, 2) precise quantification of said libraries for optimal loading on
612 the sequencing instrument, and 3) large batch sizes (samples in increments of 96, 192, or larger to
613 accommodate the capacity of the intended sequencing instrument).

614 Though these AmpSeq protocols share many common features, they differ in other aspects that
615 may impact implementation. Whereas the 4CAST and Paragon panels and single nested PCR reactions
616 perform well on native DNA from clinical samples, the AMPLseq and SpotMalaria panels require sWGA
617 pre-amplification prior to the first PCR reaction to ensure adequate performance for samples with
618 parasitemia at or below 100 parasites/ μ l, which may comprise a significant proportion of samples in
619 some settings. sWGA is an isothermal amplification protocol that is relatively simple to perform but
620 requires an expensive phi29 DNA polymerase and a magnetic bead-based cleanup of individual samples
621 afterward, for an approximate additional cost of \$8 USD per sample at the time of writing. Though not

622 large in absolute terms, this cost is comparable to the cost of the AMPLseq or 4CAST protocols
623 themselves, which range from \$5 – 10 USD per sample, depending on details of implementation such as
624 sequencing instrument and sample indexing per run. The larger panels additionally employ differing
625 numbers of first-round PCR reactions and require a varying number of magnetic bead-based cleanups to
626 tailor the length profile of intermediate products (summarized in **S5 Table**), which means that the local
627 capacity for automating the bead-based cleanups is a relevant implementation consideration.

628 The third criterion for panel selection, customizability, may be most relevant for the drug
629 resistance surveillance use case, given differences in the geographic distribution of important drug
630 markers, and varying coverage of known markers by the existing panels. All of the protocols are
631 amenable to customization through the addition of independent target amplifications in the first round of
632 PCR, which could be combined with other first-round PCR multiplex products prior to the second PCR. A
633 more elegant customization approach would be to add (or subtract) targets from the first-round PCR
634 reaction. While complicated bioinformatic pipelines are useful or essential in the design of large
635 multiplexes, in our experience, small multiplexes like 4CAST, which was made from pre-existing primer
636 pairs designed independently, may simply function without optimization, and could presumably be
637 augmented with a small number of additional loci. Though the AMPLseq multiplex of 129 PCR loci
638 benefited from careful design of the original panel, we added the 4CAST targets to the designed
639 AMPLseq target set with no primer modifications and found it to be functional, suggesting it is likely
640 receptive to further augmentation. As the AMPLseq and 4CAST protocols utilize unmodified,
641 commercially available oligos as primers, further customization should be feasible in any setting.
642 However, we must note that not all targets are amenable to incorporation into the multiplex, as we failed
643 despite multiple attempts to include amplicons targeting the *pfcr*t gene associated with chloroquine
644 resistance (Fidock et al., 2000), or the *hrp2/3* genes, which can contain deletions that lead to
645 false-negative diagnosis via rapid diagnostic test (Gamboa et al., 2010).

646 The proliferation of new AmpSeq protocols for molecular surveillance of infectious diseases
647 raises the important question of whether it is valuable for each disease field to converge on a single
648 approach or common panel. Factors precluding a completely homogeneous approach include varying

649 instrumentation, expertise, and use cases for the data across settings, in addition to an anticipated
650 onward evolution of genotyping technology and elucidation of new markers of interest for drug resistance
651 or other phenotypes. Factors favoring convergence include opportunities for improved procurement of
652 instruments and reagents at a regional level in malaria-endemic countries, and opportunities to directly
653 compare observations between studies and surveillance efforts led by different groups. This latter factor,
654 which we term portability of analyses, has the potential to provide regional or global insight through
655 syntheses across studies. However, the portability of certain analyses is hampered by ascertainment
656 bias, an inherent limitation of any targeted sequencing approach for analyses based on the genotypic
657 state of select loci in different countries. That is, a panel designed based on observations of genetic
658 diversity through WGS in countries A and B may not provide a fair means of comparing diversity in
659 countries C vs. D, if diversity there is distributed differently in the genome than in countries A and B.
660 WGS is the ultimate tool for avoiding this bias. However, the problems of comparing parasite populations
661 profiled with different panels may be mitigated by comparing inferred relatedness levels within
662 populations rather than actual genotypic diversity measures. Overlap of loci among panels would further
663 facilitate direct assessment of relatedness between samples included in different studies (Neafsey,
664 Taylor, & MacInnis, 2021; Taylor et al., 2019). The AMPLseq panel we describe here contains a
665 significant number (n=47) of targets from the SpotMalaria panel, and we expect that future *P. falciparum*
666 panel designs will also tend to exhibit some degree of overlap with other panels, both by deliberate
667 design and through blind convergence based on key genomic features, such as high diversity and
668 sequence amenability to PCR primer design.

669 As molecular surveillance efforts for malaria and other diseases are more widely adopted and
670 become increasingly diverse, it will be essential for the community to develop standardized approaches
671 for the design, validation, interpretation, and sharing of targeted amplicon sequencing data. The
672 paneljudge R package described here provides an excellent means to comparatively evaluate existing
673 and hypothetical panel performance via data collected from previous population genomic surveys, and
674 the bioinformatic analysis pipelines we have developed are suitable for interpreting Illumina data from
675 diverse targets and panels in different organisms. We anticipate the growth of this field and the

676 development of new analytical tools to extract even more knowledge from increasingly large AmpSeq
677 datasets.

678 **Acknowledgments**

679 This project has been funded in whole or in part with Federal funds from the National Institute of
680 Allergy and Infectious Diseases, National Institutes of Health, Department of Health and Human
681 Services, under Grant Number U19AI110818 to the Broad Institute. This project was also supported by
682 an NIH R01 award to DN (R01AI141544), an award from the Bill and Melinda Gates Foundation to DN
683 and COB (OPP1213366), and a Broad Institute NextGen Award to BM. The Mali cohort study was
684 funded by the Division of Intramural Research, National Institute of Allergy and Infectious Diseases,
685 National Institutes of Health. The Colombian cohort study was supported by British Council
686 Newton-Caldas Fund Institutional Links Award G1854. We thank MalariaGen for use of the Colombian
687 WGS data. We thank Annie Laws for project management. We thank Dr. Nathan Campbell for assistance
688 in the AMPLseq panel design and evaluation.

689 **Data Accessibility and Benefit Sharing**

690 Data Accessibility: All amplicon sequencing data, as well as WGS data from 16 Guyana samples,
691 were submitted to the NCBI Sequence Read Archive (<http://www.ncbi.nlm.nih.gov/sra>) under accession
692 PRJNA758191. This publication uses data from the MalariaGEN Plasmodium falciparum Community
693 Project as described online pending publication and public release of dataset Pf7
694 (<https://www.malariagen.net/resource/34>); additional ENA accession numbers are available in Table S4.
695 Previously published data from Guyana and French Guiana can be found at SRA BioProjects
696 PRJNA543530 and PRJNA242182, respectively. Software and documentation can be found at
697 <https://github.com/broadinstitute/AmpSeQC> (AmpSeQC pipeline),
698 <https://github.com/broadinstitute/malaria-amplicon-pipeline.git> (Malaria amplicon pipeline), and
699 <https://github.com/artaylor85/paneljudge> (paneljudge).

700 Benefits Generated: A research collaboration was developed with scientists from the countries
701 providing genetic samples, all collaborators are included as co-authors, the results of research have

702 been shared with the provider communities and the broader scientific community (see above), and the
703 research addresses a priority concern, in this case the public health concern of malaria. More broadly,
704 our group is committed to international scientific partnerships, as well as institutional capacity building.

705 **Author Contributions**

- 706 ● Conceptualization EL, PS, MC, ART, AME, BLM, DEN
- 707 ● Data Curation ZMJ, RP, TJS
- 708 ● Formal Analysis EL, PS, MC, ART, RP, TJS
- 709 ● Funding Acquisition COB, BLM, DEN
- 710 ● Investigation PS, MC, ZMJ, MS, RK, SW
- 711 ● Methodology EL, MC, PS, ART, ZMJ, MS, RP, TJS, RK
- 712 ● Project Administration BLM, DEN
- 713 ● Resources CMA, SP, PDC, BT, JCR, VC, KJ, HC
- 714 ● Software ART, RP, TJS, AME
- 715 ● Supervision COB, BLM, AME, DEN
- 716 ● Validation EL, PS, MC, ZMJ, MS, RP, TJS, RK
- 717 ● Visualization EL, PS, MC, ART, RP
- 718 ● Writing - Original Draft Preparation EL, PS, MC, ART, DEN
- 719 ● Writing - Review & Editing [All authors]

720 **References**

- 721 Arie, F., Witkowski, B., Amaratunga, C., Beghain, J., Langlois, A.-C., Khim, N., Kim, S., Duru, V.,
722 Bouchier, C., Ma, L., Lim, P., Leang, R., Duong, S., Sreng, S., Suon, S., Chuor, C. M., Bout, D.
723 M., Ménard, S., Rogers, W. O., ... Ménard, D. (2014). A molecular marker of artemisinin-resistant
724 *Plasmodium falciparum* malaria. *Nature*, *505*(7481), 50–55. <https://doi.org/10.1038/nature12876>
- 725 Aydemir, O., Janko, M., Hathaway, N. J., Verity, R., Mwandagalirwa, M. K., Tshefu, A. K., Tessema, S. K.,
726 Marsh, P. W., Tran, A., Reimonn, T., Ghani, A. C., Ghansah, A., Juliano, J. J., Greenhouse, B. R.,
727 Emch, M., Meshnick, S. R., & Bailey, J. A. (2018). Drug-Resistance and Population Structure of
728 *Plasmodium falciparum* Across the Democratic Republic of Congo Using High-Throughput
729 Molecular Inversion Probes. *The Journal of Infectious Diseases*, *218*(6), 946–955.
730 <https://doi.org/10.1093/infdis/jiy223>
- 731 Baetscher, D. S., Clemento, A. J., Ng, T. C., Anderson, E. C., & Garza, J. C. (2018). Microhaplotypes
732 provide increased power from short-read DNA sequences for relationship inference. *Molecular*
733 *Ecology Resources*, *18*(2), 296–305. <https://doi.org/10.1111/1755-0998.12737>
- 734 Baker, S., Thomson, N., Weill, F.-X., & Holt, K. E. (2018). Genomic insights into the emergence and
735 spread of antimicrobial-resistant bacterial pathogens. *Science*, *360*(6390), 733–738.
736 <https://doi.org/10.1126/science.aar3777>
- 737 Baniecki, M. L., Faust, A. L., Schaffner, S. F., Park, D. J., Galinsky, K., Daniels, R. F., Hamilton, E.,
738 Ferreira, M. U., Karunaweera, N. D., Serre, D., Zimmerman, P. A., Sá, J. M., Wellems, T. E.,
739 Musset, L., Legrand, E., Melnikov, A., Neafsey, D. E., Volkman, S. K., Wirth, D. F., & Sabeti, P. C.
740 (2015). Development of a single nucleotide polymorphism barcode to genotype *Plasmodium*
741 *vivax* infections. *PLoS Neglected Tropical Diseases*, *9*(3), e0003539.
742 <https://doi.org/10.1371/journal.pntd.0003539>
- 743 Callahan, B. J., McMurdie, P. J., Rosen, M. J., Han, A. W., Johnson, A. J. A., & Holmes, S. P. (2016).
744 DADA2: High-resolution sample inference from Illumina amplicon data. *Nature Methods*, *13*(7),
745 581–583. <https://doi.org/10.1038/nmeth.3869>
- 746 Campbell, N. R., Harmon, S. A., & Narum, S. R. (2015). Genotyping-in-Thousands by sequencing
747 (GT-seq): A cost effective SNP genotyping method based on custom amplicon sequencing.
748 *Molecular Ecology Resources*, *15*(4), 855–867. <https://doi.org/10.1111/1755-0998.12357>
- 749 Cerqueira, G. C., Cheeseman, I. H., Schaffner, S. F., Nair, S., McDew-White, M., Phyto, A. P., Ashley, E.
750 A., Melnikov, A., Rogov, P., Birren, B. W., Nosten, F., Anderson, T. J. C., & Neafsey, D. E. (2017).
751 Longitudinal genomic surveillance of *Plasmodium falciparum* malaria parasites reveals complex
752 genomic architecture of emerging artemisinin resistance. *Genome Biology*, *18*(1), 78.
753 <https://doi.org/10.1186/s13059-017-1204-4>
- 754 Chang, H.-H., Wesolowski, A., Sinha, I., Jacob, C. G., Mahmud, A., Uddin, D., Zaman, S. I., Hossain, M.
755 A., Faiz, M. A., Ghose, A., Sayeed, A. A., Rahman, M. R., Islam, A., Karim, M. J., Rezwana, M. K.,
756 Shamsuzzaman, A. K. M., Jhora, S. T., Aktaruzzaman, M. M., Drury, E., ... Buckee, C. (2019).
757 Mapping imported malaria in Bangladesh using parasite genetic and human mobility data. *eLife*,
758 *8*, e43481. <https://doi.org/10.7554/eLife.43481>
- 759 Chang, H.-H., Worby, C. J., Yeka, A., Nankabirwa, J., Kanya, M. R., Staedke, S. G., Dorsey, G., Murphy,
760 M., Neafsey, D. E., Jeffreys, A. E., Hubbart, C., Rockett, K. A., Amato, R., Kwiatkowski, D. P.,
761 Buckee, C. O., & Greenhouse, B. (2017). THE REAL McCOIL: A method for the concurrent
762 estimation of the complexity of infection and SNP allele frequency for malaria parasites. *PLoS*
763 *Computational Biology*, *13*(1), e1005348. <https://doi.org/10.1371/journal.pcbi.1005348>
- 764 Chenet, S. M., Akinyi Okoth, S., Huber, C. S., Chandrabose, J., Lucchi, N. W., Talundzic, E., Krishnalall,
765 K., Ceron, N., Musset, L., Macedo de Oliveira, A., Venkatesan, M., Rahman, R., Barnwell, J. W.,
766 & Udhayakumar, V. (2016). Independent Emergence of the *Plasmodium falciparum* Kelch
767 Propeller Domain Mutant Allele C580Y in Guyana. *The Journal of Infectious Diseases*, *213*(9),
768 1472–1475. <https://doi.org/10.1093/infdis/jiv752>
- 769 Chenet, S. M., Okoth, S. A., Kelley, J., Lucchi, N., Huber, C. S., Vreden, S., Macedo de Oliveira, A.,
770 Barnwell, J. W., Udhayakumar, V., & Adhin, M. R. (2017). Molecular Profile of Malaria Drug
771 Resistance Markers of *Plasmodium falciparum* in Suriname. *Antimicrobial Agents and*
772 *Chemotherapy*, *61*(7), e02655-16. <https://doi.org/10.1128/AAC.02655-16>
- 773 Coll, F., Harrison, E. M., Toleman, M. S., Reuter, S., Raven, K. E., Blane, B., Palmer, B., Kappeler, A. R.

- 774 M., Brown, N. M., Török, M. E., Parkhill, J., & Peacock, S. J. (2017). Longitudinal genomic
775 surveillance of MRSA in the UK reveals transmission patterns in hospitals and the community.
776 *Science Translational Medicine*, 9(413), eaak9745. <https://doi.org/10.1126/scitranslmed.aak9745>
- 777 Dalmat, R., Naughton, B., Kwan-Gett, T. S., Slyker, J., & Stuckey, E. M. (2019). Use cases for genetic
778 epidemiology in malaria elimination. *Malaria Journal*, 18(1), 1–11.
779 <https://doi.org/10.1186/s12936-019-2784-0>
- 780 Danecek, P., Auton, A., Abecasis, G., Albers, C. A., Banks, E., DePristo, M. A., Handsaker, R. E., Lunter,
781 G., Marth, G. T., Sherry, S. T., McVean, G., Durbin, R., & 1000 Genomes Project Analysis Group.
782 (2011). The variant call format and VCFtools. *Bioinformatics*, 27(15), 2156–2158.
783 <https://doi.org/10.1093/bioinformatics/btr330>
- 784 Daniels, R. F., Schaffner, S. F., Wenger, E. A., Proctor, J. L., Chang, H.-H., Wong, W., Baro, N., Ndiaye,
785 D., Fall, F. B., Ndiop, M., Ba, M., Milner, D. A., Taylor, T. E., Neafsey, D. E., Volkman, S. K.,
786 Eckhoff, P. A., Hartl, D. L., & Wirth, D. F. (2015). Modeling malaria genomics reveals transmission
787 decline and rebound in Senegal. *Proceedings of the National Academy of Sciences of the United*
788 *States of America*, 112(22), 7067–7072. <https://doi.org/10.1073/pnas.1505691112>
- 789 Daniels, R., Volkman, S. K., Milner, D. A., Mahesh, N., Neafsey, D. E., Park, D. J., Rosen, D., Angelino,
790 E., Sabeti, P. C., Wirth, D. F., & Wiegand, R. C. (2008). A general SNP-based molecular barcode
791 for *Plasmodium falciparum* identification and tracking. *Malaria Journal*, 7, 223.
792 <https://doi.org/10.1186/1475-2875-7-223>
- 793 DePristo, M. A., Banks, E., Poplin, R., Garimella, K. V., Maguire, J. R., Hartl, C., Philippakis, A. A., del
794 Angel, G., Rivas, M. A., Hanna, M., McKenna, A., Fennell, T. J., Kernysky, A. M., Sivachenko, A.
795 Y., Cibulskis, K., Gabriel, S. B., Altshuler, D., & Daly, M. J. (2011). A framework for variation
796 discovery and genotyping using next-generation DNA sequencing data. *Nature Genetics*, 43(5),
797 491–498. <https://doi.org/10.1038/ng.806>
- 798 Early, A. M., Daniels, R. F., Farrell, T. M., Grimsby, J., Volkman, S. K., Wirth, D. F., MacInnis, B. L., &
799 Neafsey, D. E. (2019). Detection of low-density *Plasmodium falciparum* infections using amplicon
800 deep sequencing. *Malaria Journal*, 18(1), 219. <https://doi.org/10.1186/s12936-019-2856-1>
- 801 Fidock, D. A., Nomura, T., Talley, A. K., Cooper, R. A., Dzekunov, S. M., Ferdig, M. T., Ursos, L. M.,
802 Sidhu, A. B., Naudé, B., Deitsch, K. W., Su, X. Z., Wootton, J. C., Roepe, P. D., & Wellems, T. E.
803 (2000). Mutations in the *P. falciparum* digestive vacuole transmembrane protein PfCRT and
804 evidence for their role in chloroquine resistance. *Molecular Cell*, 6(4), 861–871.
805 [https://doi.org/10.1016/s1097-2765\(05\)00077-8](https://doi.org/10.1016/s1097-2765(05)00077-8)
- 806 Fola, A. A., Kattenberg, E., Razook, Z., Lautu-Gumal, D., Lee, S., Mehra, S., Bahlo, M., Kazura, J.,
807 Robinson, L. J., Laman, M., Mueller, I., & Barry, A. E. (2020). SNP barcodes provide higher
808 resolution than microsatellite markers to measure *Plasmodium vivax* population genetics. *Malaria*
809 *Journal*, 19(1), 375. <https://doi.org/10.1186/s12936-020-03440-0>
- 810 Galinsky, K., Valim, C., Salmier, A., de Thoisy, B., Musset, L., Legrand, E., Faust, A., Baniecki, M.,
811 Ndiaye, D., Daniels, R. F., Hartl, D. L., Sabeti, P. C., Wirth, D. F., Volkman, S. K., & Neafsey, D. E.
812 (2015). COIL: a methodology for evaluating malarial complexity of infection using likelihood from
813 single nucleotide polymorphism data. *Malaria Journal*, 14(1), 4.
814 <https://doi.org/10.1186/1475-2875-14-4>
- 815 Gamboa, D., Ho, M.-F., Bendezu, J., Torres, K., Chiodini, P. L., Barnwell, J. W., Incardona, S., Perkins,
816 M., Bell, D., McCarthy, J., & Cheng, Q. (2010). A Large Proportion of *P. falciparum* Isolates in the
817 Amazon Region of Peru Lack pfrp2 and pfrp3: Implications for Malaria Rapid Diagnostic Tests.
818 *PloS One*, 5(1). <https://doi.org/10.1371/journal.pone.0008091>
- 819 Gruenberg, M., Lerch, A., Beck, H.-P., & Felger, I. (2019). Amplicon deep sequencing improves
820 *Plasmodium falciparum* genotyping in clinical trials of antimalarial drugs. *Scientific Reports*, 9(1),
821 1–12. <https://doi.org/10.1038/s41598-019-54203-0>
- 822 Hargrove, J. S., McCane, J., Roth, C. J., High, B., & Campbell, M. R. (2021). Mating systems and
823 predictors of relative reproductive success in a Cutthroat Trout subspecies of conservation
824 concern. *Ecology and Evolution*, 11(16). <https://doi.org/10.1002/ece3.7914>
- 825 Helb, D. A., Tetteh, K. K. A., Felgner, P. L., Skinner, J., Hubbard, A., Arinaitwe, E., Mayanja-Kizza, H.,
826 Ssewanyana, I., Kamya, M. R., Beeson, J. G., Tappero, J., Smith, D. L., Crompton, P. D.,
827 Rosenthal, P. J., Dorsey, G., Drakeley, C. J., & Greenhouse, B. (2015). Novel serologic

- 828 biomarkers provide accurate estimates of recent *Plasmodium falciparum* exposure for individuals
829 and communities. *Proceedings of the National Academy of Sciences*, 112(32), E4438–E4447.
830 <https://doi.org/10.1073/pnas.1501705112>
- 831 Henden, L., Lee, S., Mueller, I., Barry, A., & Bahlo, M. (2018). Identity-by-descent analyses for measuring
832 population dynamics and selection in recombining pathogens. *PLoS Genetics*, 14(5), e1007279.
833 <https://doi.org/10.1371/journal.pgen.1007279>
- 834 Jacob, C. G., Thuy-Nhien, N., Mayxay, M., Maude, R. J., Quang, H. H., Hongvanthong, B., Vanisaveth,
835 V., Ngo Duc, T., Rekol, H., van der Pluijm, R., von Seidlein, L., Fairhurst, R., Nosten, F., Hossain,
836 M. A., Park, N., Goodwin, S., Ringwald, P., Chindavongsa, K., Newton, P., ... Miotto, O. (2021).
837 Genetic surveillance in the Greater Mekong subregion and South Asia to support malaria control
838 and elimination. *ELife*, 10, e62997. <https://doi.org/10.7554/eLife.62997>
- 839 Jones, S., Kay, K., Hodel, E. M., Gruenberg, M., Lerch, A., Felger, I., & Hastings, I. (2021). Should
840 deep-sequenced amplicons become the new gold-standard for analysing malaria drug clinical
841 trials? *Antimicrobial Agents and Chemotherapy*, AAC0043721.
842 <https://doi.org/10.1128/AAC.00437-21>
- 843 Kayiba, N. K., Yobi, D. M., Tshibangu-Kabamba, E., Tuan, V. P., Yamaoka, Y., Devleeschauwer, B.,
844 Mvumbi, D. M., Okitolonda Wemakoy, E., De Mol, P., Mvumbi, G. L., Hayette, M.-P.,
845 Rosas-Aguirre, A., & Speybroeck, N. (2021). Spatial and molecular mapping of Pfk13 gene
846 polymorphism in Africa in the era of emerging *Plasmodium falciparum* resistance to artemisinin: a
847 systematic review. *The Lancet. Infectious Diseases*, 21(4), e82–e92.
848 [https://doi.org/10.1016/S1473-3099\(20\)30493-X](https://doi.org/10.1016/S1473-3099(20)30493-X)
- 849 Knudson, A., González-Casabianca, F., Feged-Rivadeneira, A., Pedreros, M. F., Aponte, S., Olaya, A.,
850 Castillo, C. F., Mancilla, E., Piamba-Dorado, A., Sanchez-Pedraza, R., Salazar-Terreros, M. J.,
851 Lucchi, N., Udhayakumar, V., Jacob, C., Pance, A., Carrasquilla, M., Apráez, G., Angel, J. A.,
852 Rayner, J. C., & Corredor, V. (2020). Spatio-temporal dynamics of *Plasmodium falciparum*
853 transmission within a spatial unit on the Colombian Pacific Coast. *Scientific Reports*, 10(1), 3756.
854 <https://doi.org/10.1038/s41598-020-60676-1>
- 855 Krijthe, J. H. (2015). *Rtsne: T-Distributed Stochastic Neighbor Embedding using a Barnes-Hut*
856 *Implementation*. <https://github.com/jkrijthe/Rtsne>
- 857 Lautu-Gumal, D., Razook, Z., Koleala, T., Nate, E., McEwen, S., Timbi, D., Hetzel, M. W., Lavu, E.,
858 Tefuarani, N., Makita, L., Kazura, J., Mueller, I., Pomat, W., Laman, M., Robinson, L. J., & Barry,
859 A. E. (2021). Surveillance of molecular markers of *Plasmodium falciparum* artemisinin resistance
860 (kelch13 mutations) in Papua New Guinea between 2016 and 2018. *International Journal for*
861 *Parasitology. Drugs and Drug Resistance*, 16, 188–193.
862 <https://doi.org/10.1016/j.ijpddr.2021.06.004>
- 863 Lefterova, M. I., Budvytiene, I., Sandlund, J., Färnert, A., & Banaei, N. (2015). Simple real-time PCR and
864 amplicon sequencing method for identification of plasmodium species in human whole blood.
865 *Journal of Clinical Microbiology*, 53(7), 2251–2257. <https://doi.org/10.1128/JCM.00542-15>
- 866 Lerch, A., Koepfli, C., Hofmann, N. E., Messerli, C., Wilcox, S., Kattenberg, J. H., Betuela, I., O'Connor,
867 L., Mueller, I., & Felger, I. (2017). Development of amplicon deep sequencing markers and data
868 analysis pipeline for genotyping multi-clonal malaria infections. *BMC Genomics*, 18(1), 864.
869 <https://doi.org/10.1186/s12864-017-4260-y>
- 870 Li, H. (2013). Aligning sequence reads, clone sequences and assembly contigs with BWA-MEM.
871 *ArXiv:1303.3997 [Preprint]*. <http://arxiv.org/abs/1303.3997>
- 872 Liu, Y., Tessema, S. K., Murphy, M., Xu, S., Schwartz, A., Wang, W., Cao, Y., Lu, F., Tang, J., Gu, Y., Zhu,
873 G., Zhou, H., Gao, Q., Huang, R., Cao, J., & Greenhouse, B. (2020). Confirmation of the absence
874 of local transmission and geographic assignment of imported *falciparum* malaria cases to China
875 using microsatellite panel. *Malaria Journal*, 19(1), 244.
876 <https://doi.org/10.1186/s12936-020-03316-3>
- 877 MalariaGEN *Plasmodium falciparum* Community Project. (2016). Genomic epidemiology of artemisinin
878 resistant malaria. *ELife*, 5, e08714. <https://doi.org/10.7554/eLife.08714>
- 879 Mathieu, L. C., Cox, H., Early, A. M., Mok, S., Lazrek, Y., Paquet, J.-C., Ade, M.-P., Lucchi, N. W., Grant,
880 Q., Udhayakumar, V., Alexandre, J. S., Demar, M., Ringwald, P., Neafsey, D. E., Fidock, D. A., &
881 Musset, L. (2020). Local emergence in Amazonia of *Plasmodium falciparum* k13 C580Y mutants

- 882 associated with in vitro artemisinin resistance. *ELife*, 9, e51015.
883 <https://doi.org/10.7554/eLife.51015>
- 884 McKenna, A., Hanna, M., Banks, E., Sivachenko, A., Cibulskis, K., Kernytzky, A., Garimella, K., Altshuler,
885 D., Gabriel, S., Daly, M., & DePristo, M. A. (2010). The Genome Analysis Toolkit: a MapReduce
886 framework for analyzing next-generation DNA sequencing data. *Genome Research*, 20(9),
887 1297–1303. <https://doi.org/10.1101/gr.107524.110>
- 888 Miles, A., Iqbal, Z., Vauterin, P., Pearson, R., Campino, S., Theron, M., Gould, K., Mead, D., Drury, E.,
889 O'Brien, J., Rubio, V. R., MacInnis, B., Mwangi, J., Samarakoon, U., Ranford-Cartwright, L.,
890 Ferdig, M., Hayton, K., Su, X., Wellems, T., ... Kwiatkowski, D. (2016). Indels, structural variation,
891 and recombination drive genomic diversity in *Plasmodium falciparum*. *Genome Research*, 26(9),
892 1288–1299. <https://doi.org/10.1101/gr.203711.115>
- 893 Miles, A., pyup.io bot, Murillo, R., Ralph, P., Harding, N. J., Rahul Pisupati, Summer Rae, & Tim Millar.
894 (2020). *cggh/scikit-allel: v1.3.2*. Zenodo. <https://doi.org/10.5281/zenodo.3976233>
- 895 Miller, R. H., Hathaway, N. J., Kharabora, O., Mwandagalirwa, K., Tshetu, A., Meshnick, S. R., Taylor, S.
896 M., Juliano, J. J., Stewart, V. A., & Bailey, J. A. (2017). A deep sequencing approach to estimate
897 *Plasmodium falciparum* complexity of infection (COI) and explore apical membrane antigen 1
898 diversity. *Malaria Journal*, 16(1), 490. <https://doi.org/10.1186/s12936-017-2137-9>
- 899 Miotto, O., Amato, R., Ashley, E. A., MacInnis, B., Almagro-Garcia, J., Amaratunga, C., Lim, P., Mead,
900 D., Oyola, S. O., Dhorda, M., Imwong, M., Woodrow, C., Manske, M., Stalker, J., Drury, E.,
901 Campino, S., Amenga-Etego, L., Thanh, T.-N. N., Tran, H. T., ... Kwiatkowski, D. P. (2015).
902 Genetic architecture of artemisinin-resistant *Plasmodium falciparum*. *Nature Genetics*, 47(3),
903 226–234. <https://doi.org/10.1038/ng.3189>
- 904 Miotto, O., Sekihara, M., Tachibana, S.-I., Yamauchi, M., Pearson, R. D., Amato, R., Gonçalves, S.,
905 Mehra, S., Noviyanti, R., Marfurt, J., Auburn, S., Price, R. N., Mueller, I., Ikeda, M., Mori, T., Hirai,
906 M., Tavul, L., Hetzel, M. W., Laman, M., ... Mita, T. (2020). Emergence of artemisinin-resistant
907 *Plasmodium falciparum* with kelch13 C580Y mutations on the island of New Guinea. *PLoS*
908 *Pathogens*, 16(12), e1009133. <https://doi.org/10.1371/journal.ppat.1009133>
- 909 Mita, T., Tanabe, K., Takahashi, N., Tsukahara, T., Eto, H., Dysoley, L., Ohmae, H., Kita, K., Krudsood,
910 S., Looareesuwan, S., Kaneko, A., Björkman, A., & Kobayakawa, T. (2007). Independent
911 Evolution of Pyrimethamine Resistance in *Plasmodium falciparum* Isolates in Melanesia.
912 *Antimicrobial Agents and Chemotherapy*, 51(3), 1071–1077.
913 <https://doi.org/10.1128/AAC.01186-06>
- 914 Mitchell, R. M., Zhou, Z., Sheth, M., Sergeant, S., Frace, M., Nayak, V., Hu, B., Gimnig, J., ter Kuile, F.,
915 Lindblade, K., Slutsker, L., Hamel, M. J., Desai, M., Otieno, K., Kariuki, S., Vigfusson, Y., & Shi, Y.
916 P. (2021). Development of a new barcode-based, multiplex-PCR, next-generation-sequencing
917 assay and data processing and analytical pipeline for multiplicity of infection detection of
918 *Plasmodium falciparum*. *Malaria Journal*, 20(1), 92. <https://doi.org/10.1186/s12936-021-03624-2>
- 919 Moser, K. A., Madebe, R. A., Aydemir, O., Chiduo, M. G., Mandara, C. I., Rumisha, S. F., Chaky, F.,
920 Denton, M., Marsh, P. W., Verity, R., Watson, O. J., Ngasala, B., Mkude, S., Molteni, F., Njau, R.,
921 Warsame, M., Mandike, R., Kabanywany, A. M., Mahende, M. K., ... Bailey, J. A. (2021).
922 Describing the current status of *Plasmodium falciparum* population structure and drug resistance
923 within mainland Tanzania using molecular inversion probes. *Molecular Ecology*, 30(1), 100–113.
924 <https://doi.org/10.1111/mec.15706>
- 925 Natesh, M., Taylor, R. W., Truelove, N. K., Hadly, E. A., Palumbi, S. R., Petrov, D. A., & Ramakrishnan,
926 U. (2019). Empowering conservation practice with efficient and economical genotyping from poor
927 quality samples. *Methods in Ecology and Evolution*, 10(6), 853–859.
928 <https://doi.org/10.1111/2041-210X.13173>
- 929 Neafsey, D. E., Juraska, M., Bedford, T., Benkeser, D., Valim, C., Griggs, A., Lievens, M., Abdulla, S.,
930 Adjei, S., Agbenyega, T., Agnandji, S. T., Aide, P., Anderson, S., Ansong, D., Aponte, J. J.,
931 Asante, K. P., Bejon, P., Birkett, A. J., Bruls, M., ... Wirth, D. F. (2015). Genetic Diversity and
932 Protective Efficacy of the RTS,S/AS01 Malaria Vaccine. *New England Journal of Medicine*,
933 373(21), 2025–2037. <https://doi.org/10.1056/NEJMoa1505819>
- 934 Neafsey, D. E., Taylor, A. R., & MacInnis, B. L. (2021). Advances and opportunities in malaria population
935 genomics. *Nature Reviews. Genetics*. <https://doi.org/10.1038/s41576-021-00349-5>

- 936 Nelson, C. S., Sumner, K. M., Freedman, E., Saelens, J. W., Obala, A. A., Mangeni, J. N., Taylor, S. M.,
937 & O'Meara, W. P. (2019). High-resolution micro-epidemiology of parasite spatial and temporal
938 dynamics in a high malaria transmission setting in Kenya. *Nature Communications*, *10*, 5615.
939 <https://doi.org/10.1038/s41467-019-13578-4>
- 940 Oude Munnink, B. B., Worp, N., Nieuwenhuijse, D. F., Sikkema, R. S., Haagmans, B., Fouchier, R. A. M.,
941 & Koopmans, M. (2021). The next phase of SARS-CoV-2 surveillance: real-time molecular
942 epidemiology. *Nature Medicine*. <https://doi.org/10.1038/s41591-021-01472-w>
- 943 Oyola, S. O., Ariani, C. V., Hamilton, W. L., Kekre, M., Amenga-Etego, L. N., Ghansah, A., Rutledge, G.
944 G., Redmond, S., Manske, M., Jyothi, D., Jacob, C. G., Otto, T. D., Rockett, K., Newbold, C. I.,
945 Berriman, M., & Kwiatkowski, D. P. (2016). Whole genome sequencing of *Plasmodium falciparum*
946 from dried blood spots using selective whole genome amplification. *Malaria Journal*, *15*(1).
947 <https://doi.org/10.1186/s12936-016-1641-7>
- 948 Pelleau, S., Moss, E. L., Dhingra, S. K., Volney, B., Casteras, J., Gabryszewski, S. J., Volkman, S. K.,
949 Wirth, D. F., Legrand, E., Fidock, D. A., Neafsey, D. E., & Musset, L. (2015). Adaptive evolution of
950 malaria parasites in French Guiana: Reversal of chloroquine resistance by acquisition of a
951 mutation in *pfcr*. *Proceedings of the National Academy of Sciences*, *112*(37), 11672–11677.
952 <https://doi.org/10.1073/pnas.1507142112>
- 953 Quick, J., Loman, N. J., Duraffour, S., Simpson, J. T., Severi, E., Cowley, L., Bore, J. A., Koundouno, R.,
954 Dudas, G., Mikhail, A., Ouédraogo, N., Afrough, B., Bah, A., Baum, J. H. J., Becker-Ziaja, B.,
955 Boettcher, J. P., Cabeza-Cabrero, M., Camino-Sánchez, Á., Carter, L. L., ... Carroll, M. W.
956 (2016). Real-time, portable genome sequencing for Ebola surveillance. *Nature*, *530*(7589),
957 228–232. <https://doi.org/10.1038/nature16996>
- 958 Reeder, J. C., & Marshall, V. M. (1994). A simple method for typing *Plasmodium falciparum* merozoite
959 surface antigens 1 and 2 (MSA-1 and MSA-2) using a dimorphic-form specific polymerase chain
960 reaction. *Molecular and Biochemical Parasitology*, *68*(2), 329–332.
961 [https://doi.org/10.1016/0166-6851\(94\)90179-1](https://doi.org/10.1016/0166-6851(94)90179-1)
- 962 Ruybal-Pesántez, S., Sáenz, F. E., Deed, S., Johnson, E. K., Larremore, D. B., Vera-Arias, C. A., Tiedje,
963 K. E., & Day, K. P. (2021). Clinical malaria incidence following an outbreak in Ecuador was
964 predominantly associated with *Plasmodium falciparum* with recombinant variant antigen gene
965 repertoires. *MedRxiv [Preprint]*, 2021.04.12.21255093.
966 <https://doi.org/10.1101/2021.04.12.21255093>
- 967 Schaffner, S. F., Taylor, A. R., Wong, W., Wirth, D. F., & Neafsey, D. E. (2018). hmmlBD: software to infer
968 pairwise identity by descent between haploid genotypes. *Malaria Journal*, *17*(1), 196.
969 <https://doi.org/10.1186/s12936-018-2349-7>
- 970 Schmidt, D. A., Campbell, N. R., Govindarajulu, P., Larsen, K. W., & Russello, M. A. (2020).
971 Genotyping-in-Thousands by sequencing (GT-seq) panel development and application to
972 minimally invasive DNA samples to support studies in molecular ecology. *Molecular Ecology*
973 *Resources*, *20*(1), 114–124. <https://doi.org/10.1111/1755-0998.13090>
- 974 Schwabl, P., Maignashca Sánchez, J., Costales, J. A., Ocaña-Mayorga, S., Segovia, M., Carrasco, H. J.,
975 Hernández, C., Ramírez, J. D., Lewis, M. D., Grijalva, M. J., & Llewellyn, M. S. (2020).
976 Culture-free genome-wide locus sequence typing (GLST) provides new perspectives on
977 *Trypanosoma cruzi* dispersal and infection complexity. *PLoS Genetics*, *16*(12), e1009170.
978 <https://doi.org/10.1371/journal.pgen.1009170>
- 979 Snounou, G. (2002). Genotyping of *Plasmodium* spp. Nested PCR. *Methods in Molecular Medicine*, *72*,
980 103–116. <https://doi.org/10.1385/1-59259-271-6:103>
- 981 Takala-Harrison, S., Jacob, C. G., Arze, C., Cummings, M. P., Silva, J. C., Dondorp, A. M., Fukuda, M.
982 M., Hien, T. T., Mayxay, M., Noedl, H., Nosten, F., Kyaw, M. P., Nhien, N. T. T., Imwong, M.,
983 Bethell, D., Se, Y., Lon, C., Tyner, S. D., Saunders, D. L., ... Plowe, C. V. (2015). Independent
984 emergence of artemisinin resistance mutations among *Plasmodium falciparum* in Southeast Asia.
985 *The Journal of Infectious Diseases*, *211*(5), 670–679. <https://doi.org/10.1093/infdis/jiu491>
- 986 Taylor, A. R., & Jacob, P. E. (2020). *paneljudge: Judge the performance of a panel of genetic markers*
987 *using simulated data*. (R package version 0.0.0.9000) [Computer software].
- 988 Taylor, A. R., Jacob, P. E., Neafsey, D. E., & Buckee, C. O. (2019). Estimating Relatedness Between
989 Malaria Parasites. *Genetics*, *212*(4), 1337–1351. <https://doi.org/10.1534/genetics.119.302120>

- 990 Taylor, A. R., Schaffner, S. F., Cerqueira, G. C., Nkhoma, S. C., Anderson, T. J. C., Sriprawat, K., Pyae
991 Phyo, A., Nosten, F., Neafsey, D. E., & Buckee, C. O. (2017). Quantifying connectivity between
992 local *Plasmodium falciparum* malaria parasite populations using identity by descent. *PLoS*
993 *Genetics*, *13*(10), e1007065. <https://doi.org/10.1371/journal.pgen.1007065>
- 994 Taylor, S. M., Parobek, C. M., DeConti, D. K., Kayentao, K., Coulibaly, S. O., Greenwood, B. M., Tagbor,
995 H., Williams, J., Bojang, K., Njie, F., Desai, M., Kariuki, S., Gutman, J., Mathanga, D. P.,
996 Mårtensson, A., Ngasala, B., Conrad, M. D., Rosenthal, P. J., Tshefu, A. K., ... Juliano, J. J.
997 (2015). Absence of Putative Artemisinin Resistance Mutations Among *Plasmodium falciparum* in
998 Sub-Saharan Africa: A Molecular Epidemiologic Study. *The Journal of Infectious Diseases*,
999 *211*(5), 680–688. <https://doi.org/10.1093/infdis/jiu467>
- 1000 Tessema, S. K., Hathaway, N. J., Teyssier, N. B., Murphy, M., Chen, A., Aydemir, O., Duarte, E. M.,
1001 Simone, W., Colborn, J., Saute, F., Crawford, E., Aide, P., Bailey, J. A., & Greenhouse, B. (2020).
1002 Sensitive, highly multiplexed sequencing of microhaplotypes from the *Plasmodium falciparum*
1003 heterozygote. *The Journal of Infectious Diseases*. <https://doi.org/10.1093/infdis/jiaa527>
- 1004 Tessema, S., Wesolowski, A., Chen, A., Murphy, M., Wilhelm, J., Mupiri, A.-R., Ruktanonchai, N. W.,
1005 Alegana, V. A., Tatem, A. J., Tambo, M., Didier, B., Cohen, J. M., Bennett, A., Sturrock, H. J.,
1006 Gosling, R., Hsiang, M. S., Smith, D. L., Mumbengegwi, D. R., Smith, J. L., & Greenhouse, B.
1007 (2019). Using parasite genetic and human mobility data to infer local and cross-border malaria
1008 connectivity in Southern Africa. *ELife*, *8*, e43510. <https://doi.org/10.7554/eLife.43510>
- 1009 Trager, W., & Jensen, J. B. (1976). Human malaria parasites in continuous culture. *Science (New York,*
1010 *N.Y.)*, *193*(4254), 673–675. <https://doi.org/10.1126/science.781840>
- 1011 Tran, T. M., Li, S., Doumbo, S., Doumtabe, D., Huang, C.-Y., Dia, S., Bathily, A., Sangala, J., Kone, Y.,
1012 Traore, A., Niangaly, M., Dara, C., Kayentao, K., Ongoiba, A., Doumbo, O. K., Traore, B., &
1013 Crompton, P. D. (2013). An Intensive Longitudinal Cohort Study of Malian Children and Adults
1014 Reveals No Evidence of Acquired Immunity to *Plasmodium falciparum* Infection. *Clinical*
1015 *Infectious Diseases: An Official Publication of the Infectious Diseases Society of America*, *57*(1),
1016 40–47. <https://doi.org/10.1093/cid/cit174>
- 1017 Van der Auwera, G. A., Carneiro, M. O., Hartl, C., Poplin, R., Del Angel, G., Levy-Moonshine, A., Jordan,
1018 T., Shakir, K., Roazen, D., Thibault, J., Banks, E., Garimella, K. V., Altshuler, D., Gabriel, S., &
1019 DePristo, M. A. (2013). From FastQ data to high confidence variant calls: the Genome Analysis
1020 Toolkit best practices pipeline. *Current Protocols in Bioinformatics*, *43*, 11.10.1-11.10.33.
1021 <https://doi.org/10.1002/0471250953.bi1110s43>
- 1022 Veiga, M. I., Dhingra, S. K., Henrich, P. P., Straimer, J., Gnädig, N., Uhlemann, A.-C., Martin, R. E.,
1023 Lehane, A. M., & Fidock, D. A. (2016). Globally prevalent PfMDR1 mutations modulate
1024 *Plasmodium falciparum* susceptibility to artemisinin-based combination therapies. *Nature*
1025 *Communications*, *7*(1), 11553. <https://doi.org/10.1038/ncomms11553>
- 1026 WHO. (2019). *World Malaria Report*. <https://www.who.int/publications-detail/world-malaria-report-2019>
- 1027 Zhu, S. J., Hendry, J. A., Almagro-Garcia, J., Pearson, R. D., Amato, R., Miles, A., Weiss, D. J., Lucas, T.
1028 C., Nguyen, M., Gething, P. W., Kwiatkowski, D., McVean, G., & for the Pf3k Project. (2019). The
1029 origins and relatedness structure of mixed infections vary with local prevalence of *P. falciparum*
1030 malaria. *ELife*, *8*. <https://doi.org/10.7554/eLife.40845>